Journal of Hydrology 530 (2015) 431–446

Contents lists available at ScienceDirect

Journal of Hydrology

journal homepage: www.elsevier.com/locate/jhydrol

Modeling the effects of different irrigation water salinity on soil water movement, uptake and multicomponent solute transport

E.H. Lekakis, V.Z. Antonopoulos *

Department of Hydraulics, Soil Science and Agricultural Engineering, School of Agriculture, Aristotle University of Thessaloniki, 54124 Thessaloniki, Greece

ARTICLE INFO

Article history:
Received 21 October 2014
Received in revised form 16 September 2015
Accepted 29 September 2015
Available online 9 October 2015
This manuscript was handled by Peter K. Kitanidis, Editor-in-Chief, with the assistance of Martin Thullner, Associate Editor

Keywords:
WANISIM model
Field experiment
Maize plots
Irrigation water quality
Soil salinity
Soil sodicity

SUMMARY

Simulation models can be important tools for analyzing and managing irrigation, soil salinization or crop production problems. In this study a mathematical model that describes the water movement and mass transport of individual ions (Ca^{2+}, Mg^{2+} and Na^{+}) and overall soil salinity by means of the soil solution electrical conductivity, is used. The mass transport equations of Ca^{2+}, Mg^{2+} and Na^{+} have been incorporated as part of the integrated model *WANISIM* and the soil salinity was computed as the sum of individual ions. The model was calibrated and validated against field data, collected during a three year experiment in plots of maize, irrigated with three different irrigation water qualities, at Thessaloniki area in Northern Greece. The model was also used to evaluate salinization and sodification hazards by the use of irrigation water with increasing electrical conductivity of 0.8, 3.2 and 6.4 dS m^{-1}, while maintaining a ratio of Ca^{2+}:Mg^{2+}:Na^{+} equal to 3:3:2. The qualitative and quantitative procedures for results evaluation showed that there was good agreement between the simulated and measured values of the water content, overall salinity and the concentration of individual soluble cations, at two soil layers (0–35 and 35–75 cm). Nutrient uptake was also taken into account. Locally available irrigation water (EC_{iw} = 0.8 dS m^{-1}) did not cause soil salinization or sodification. On the other hand, irrigation water with EC_{iw} equal to 3.2 and 6.4 dS m^{-1} caused severe soil salinization, but not sodification. The rainfall water during the winter seasons was not sufficient to leach salts below the soil profile of 110 cm. The modified version of model *WANISIM* is able to predict the effects of irrigation with saline waters on soil and plant growth and it is suitable for irrigation management in areas with scarce and low quality water resources.

1. Introduction

Salinity is one of the most severe environmental factors limiting the productivity of agricultural crops. About 17% of the world's cropland is under irrigation, but irrigated agriculture contributes well over 30% of the total agricultural production. Thus, secondary salinization of irrigated lands is of major concern for global food production. Estimates indicate that at least 20% of the irrigated lands are salt-affected. On the other hand, there is a limited amount of directly usable fresh water, contrasting with continuing increases in the world population and demand for fresh water. Irrigated agriculture uses about 65% of the consumed water. However, the extent of water dedicated to irrigated agriculture is likely to be challenged, as pressure is mounting to meet increased demands for human consumption and industrial uses (Ghassemi et al., 1995; Pitman and Läuchli, 2002).

In order to fill the gap between demand and supply of freshwater, agriculture in semi-arid areas will increasingly resort to using marginal-quality waters, such as urban wastewater, drainage water generated by irrigated agriculture and moderately saline surface and groundwater (Qadir et al., 2007; Oster et al., 2012). A variety of strategies have been adopted to overcome problems associated with soil salinity, including improving the productivity of saline soils mainly through leaching of excess soluble salts, blending saline with better quality waters, cyclic use of saline and non-saline waters, selecting of tolerant varieties of suitable crops and using appropriate agronomic practices (Qadir and Oster, 2004; Grattan et al., 2012).

Adoption of suitable salinity control measures requires determination of salt and water movement through the soil profile and prediction of crop response to soil water and soil salinity, subject to various climatic, soil and agronomic factors (Rasouli et al., 2013). Mathematical models that consider and integrate various climatic, crop, and edaphic factors have been suggested as useful tools for assessing the best management practices for saline conditions (Gonçalves et al., 2006; Ramos et al., 2011).

* Corresponding author.
E-mail addresses: elekakis@agro.auth.gr (E.H. Lekakis), vasanton@agro.auth.gr (V.Z. Antonopoulos).

http://dx.doi.org/10.1016/j.jhydrol.2015.09.070
0022-1694/

A large number of models for simulating water flow and solute transport in the unsaturated zone are used for a wide range of applications in research, management and risk assessment of subsurface systems. Most vadose zone models are based on the numerical solution of the Richards equation for variably-saturated water flow (transient-state models) and on analytical or numerical solutions of the Fickian-based convection–dispersion equation for solute transport. A sink term is usually included in these equations to account for root water and nutrient uptake and the effects of water and osmotic stress (Feddes and Raats, 2004). Evaluation of these models under field conditions is increasing lately, although there is need for a vast number of input data, including soil hydraulic properties, solute transport parameters, parameters characterizing the partitioning between the solid phase and the soil solution, meteorological and crop related information.

Many models have been developed over the past years that describe soil salinity through the electrical conductivity of the soil solution (EC_{sw}). EC_{sw} is determined either as an independent solute or from individual ions, available only in the liquid phase. Although the first approach severely simplifies several processes, it is incorporated in several models with acceptable results published in the literature. Models SWAP (Kroes et al., 1999), SALTMED (Ragab, 2002) and ENVIRO-GRO (Pang and Letey, 1998) use the equation of solute transport to describe EC_{sw} as an individual solute. On the other hand, models UNSATCHEM (Šimůnek et al., 1996) and HYDRUS-1D (Šimůnek et al., 2008) incorporate modules of major ions chemistry in soil, considering complex processes of adsorption and cation exchange and have proved to be very efficient in modeling major cations in the soil solution. However, these models require a vast number of input data related to physical and chemical parameters and significant computational time for the simultaneous solution of the non linear mass transport equations for every cation, in each time step.

The performance and accuracy of a medium structure model, between the two opposing approaches discussed earlier, has not yet been evaluated. Model *WANISIM* (Antonopoulos, 2001) which describes the one-dimensional water and nitrogen movement in the soil, was modified with the incorporation of modules that describe ion transport in the soil, for salinity management. The model presents medium complexity regarding the estimation of EC_{sw} as the sum of the cations in the soil solution, which is a more accurate approach, than using salinity as an independent solute. This approach is more closely related to processes occurring in the soil. Some of these processes are taken into account, and are cation exchange and distribution between the liquid and the solid phase; however, interactions between cations and complex ion chemistry are not taken into account.

The objectives of this paper were as follows: (i) the calibration, validation and evaluation of the modified *WANISIM* model to describe soil water content, concentrations of individual ions and the overall salinity given by the EC_{sw}, under field conditions, (ii) to carry out field experiments to quantify salinization and sodification risks of long term use of saline irrigation water in maize treatments, for three consecutive years and (iii) to examine the impact of salt built up and salinity on plant root water uptake.

2. Materials and methods

2.1. Model description

WANISIM model has been calibrated and evaluated under field conditions for the simulation of water, nitrogen dynamics and soil temperature (Antonopoulos and Wyseure, 1998; Antonopoulos, 1997, 2000, 2006; Rahil and Antonopoulos, 2007). The model has been modified for irrigation management under saline conditions. In the model, the concentration of each cation is calculated by the corresponding mass transport equation. Cation exchange and distribution between the liquid and the solid phase are described by the isotherm of Freundlich, in its linear form and equilibrium chemical reactions between major cations are not taken into account. In the model, EC_{sw} is calculated as the sum of the cations in the soil solution. An overview of the modifications and processes employed by model *WANISIM* is presented below.

2.1.1. Water flow

The one-dimensional vertical flow of water in the soil matrix of the unsaturated–saturated zone is described by the Richard's equation:

$$C_h \frac{\partial h}{\partial t} = \frac{\partial}{\partial z}\left\{K\left[\frac{\partial h}{\partial z} - 1\right]\right\} - S_w \tag{1}$$

where C_h is the differential soil water capacity (cm^{-1}), h is the soil water pressure head (cm), z is the vertical coordinate positive in the downward direction (cm), t is the time (h), K is the hydraulic conductivity (cm h^{-1}), S_w is the sink term for water extraction rate by plant roots (cm^3 cm^{-3} h^{-1}). The soil water retention curve, $\theta(h)$, is described by the van Genuchten (1980) model and unsaturated hydraulic conductivity, $K(h)$, is evaluated by the van Genuchten–Mualem model (van Genuchten, 1980). Preferential water flow and hysteresis of soil hydraulic properties are not considered in the model.

The sink term, S_w, is evaluated using the macroscopic approach introduced by Feddes et al. (1978). In this approach, the potential transpiration rate, T_p (cm h^{-1}), is distributed over the root zone proportionally to the root density distribution function, $\beta(z)$, and is locally reduced depending on soil moisture and salinity status through multiplication with the dimensionless stress response function, $a(h, h_o, z, t)$ (Feddes and Raats, 2004; Ramos et al., 2011):

$$S_w(h, h_o, z, t) = a(h, h_o, z, t) S_p(z, t) = a(h, h_o, z, t)\beta(z)T_p(t) \tag{2}$$

where $S_p(z, t)$ and $S_w(h, h_o, z, t)$ are the potential and actual water uptake (cm^3 cm^{-3} h^{-1}) respectively, and $a(h, h_o, z, t)$ is a dimensionless function of the soil water (h) and osmotic (h_o) pressure heads ($0 \leqslant a \leqslant 1$). The osmotic pressure head is assumed to be a linear function of EC_{sw} (US Salinity Laboratory Staff, 1954), according to:

$$h_o(\mathrm{cm}) = -360 EC_{sw}(\mathrm{dS\ m^{-1}}) \tag{3}$$

The $\beta(z)$ function is described for maize, by the equation proposed by Kang et al. (2001):

$$\beta(z, t) = 1.082 c_1 exp(-c_1 z) \tag{4}$$

where $c_1 = 2.5/z_r$, z is the soil depth and z_r is the maximum rooting depth (cm). The actual transpiration rate, T_a (cm h^{-1}), over the root depth is expressed as:

$$T_a = T_p \int_0^{z_r} a(h, h_o, z, t)\beta(z)dz \tag{5}$$

In the modified model, the combined matric and osmotic effects on water uptake are described by the multiplicative approach as follows:

$$a(h, h_o, z, t) = a(h, z, t) a(h_o, z, t) \tag{6}$$

The root water uptake reduction factor due to water stress, $a(h, z, t)$, is described according to Belmans et al. (1983) approach as:

$$\alpha(h) = 0 \quad \text{for} \quad h < h_a \text{ or } h \geqslant h_{PWP} \tag{7}$$

$$\alpha(h) = (h - h_a)/(h_{FC} - h_a) \quad \text{for} \quad h_a \leqslant h < h_{FC} \tag{8}$$

$$\alpha(h) = 1 \quad \text{for} \quad h_{FC} \leqslant h < h_{CR} \tag{9}$$

$$\alpha(h) = \frac{1/h_{PWP} - 1/h}{1/h_{PWP} - 1/h_{CR}} \quad \text{for} \quad h_{CR} \leqslant h < h_{PWP} \tag{10}$$

where h_a, h_{FC}, h_{CR} and h_{PWP} are the pressure head (in absolute values) at the aeration limit, field capacity, critical level and permanent wilting point, respectively. The threshold parameters values for maize in this study were set as −10 cm, −330 cm, −3000 cm and −15,000 cm for h_a, h_{FC}, h_{CR} and h_{PWP}, respectively (Doorenbos and Pruitt, 1977; Wesseling et al., 1991).

The root water uptake reduction function due to salinity stress, $a(h_o, z, t)$, was expressed according to Maas and Hoffman (1977), in terms of the soil solution osmotic head (Homaee et al., 2002):

$$a(h_o) = 1 - \frac{\alpha_s}{360}(h_o^* - h_o) \tag{11}$$

where h_o^* is the osmotic threshold value, 360 is a factor to convert the salinity based slope to osmotic head and α_s is the slope which indicates the percent yield decrease per unit salinity decrease. The database of Maas (1996) provides values for the threshold and slope of the salinity stress model for maize, equal to 1.7 dS m^{-1} and 0.12, respectively.

A simple compensative mechanism is used for water uptake, where uptake is allowed to continue throughout the root zone until either the potential uptake is achieved or until the entire root zone is stressed after which total uptake is dictated by the stress function. However, the actual water uptake in any discrete layer is not allowed to exceed the potential transpiration allocated to that layer, through increased water uptake, in order to meet in total the potential transpiration.

The surface boundary flux of water is the algebraic sum of irrigation or precipitation, R (cm h^{-1}), and actual evaporation, E_a (cm h^{-1}), evaluated by the model at each time step. The partitioning of potential evapotranspiration (ET_p) into potential transpiration (T_p) and soil evaporation (E_p) is calculated following the procedure described in Belmans et al. (1983) and Šimůnek et al. (2008).

2.1.2. Solute transport equations

In the modified *WANISIM* model, the soil salinity is described by means of the multicomponent estimation of the EC_{sw} from the sum of the major cations Ca^{2+}, Mg^{2+} and Na^{+} which are described by different mass transport equations. The partial differential equation governing one-dimensional advective–dispersive chemical ion transport under transient flow in a variably-saturated porous medium is defined as (Bresler et al., 1982):

$$\frac{\partial(\theta C_k + \rho_b S_k)}{\partial t} = \frac{\partial}{\partial z}\left(\theta D \frac{\partial C_k}{\partial z}\right) - \frac{\partial(q C_k)}{\partial z} + \Phi_k \tag{12}$$

where θ is the volumetric water content ($cm^3\ cm^{-3}$), C_k and S_k are ion concentrations in the liquid (mg cm^{-3}) and solid phase (mg g^{-1}), respectively, ρ_b is the soil bulk density (g cm^{-3}), q is the volumetric flux density (cm h^{-1}), D is the hydrodynamic dispersion coefficient ($cm^2\ h^{-1}$), Φ_k represents source or sink of solute and subscript k represents chemical species (Ca^{2+}, Mg^{2+} and Na^{+}). Cation exchange is described by the adsorption isotherm of Freundlich relating C_k and S_k as follows:

$$S_k = K_{d,k} C_k \tag{13}$$

where $K_{d,k}$ ($cm^3\ g^{-1}$) is the distribution coefficient of a chemical species k between the liquid and the solid phase under linear chemical distribution.

Processes such as aqueous complexation, complex cation exchange and precipitation–dissolution are not considered in the transport module. The water flow and mass transport equations are solved using a Galerkin finite element method (Huyakorn et al., 1984; Antonopoulos and Papazafiriou, 1990).

The electrical conductivity of the soil solution is determined from the total soluble cation concentration of the liquid phase (US Salinity Laboratory Staff, 1954), as follows:

$$EC_{sw}(z,t) = 10^5 \sum C_k(z,t) \tag{14}$$

where $C_k(z,t)$ is the cation concentration ($mmol_{(c)}\ L^{-1}$) and EC_{sw} is the electrical conductivity (dS m^{-1}) of the soil solution.

The model calculates EC_{sw} and the concentrations of individual ions in the soil solution. Therefore, in order to compare calculated and measured values, ion concentrations and electrical conductivity were converted from saturation extract to actual soil moisture. Various relationships have been proposed for the determination of the *EC* of the in situ soil water from the *EC* of the saturation extract (Ayers and Westcot, 1985; Skaggs et al., 2006; Letey, 2007). According to the US Salinity Laboratory Staff (1954), the saturation percentage (*SP*) of the soil paste is directly related to the field moisture range. In this study, a factor f_{SP} was used to determine the ratio of the saturation percentage (θ_{SP}) to the water content at field capacity (θ_{FC}), critical point (θ_{CR}) and wilting point (θ_{PWP}), respectively. The θ_{SP} was defined by the following equation (Miller and Curtin, 2008):

$$\theta_{SP} = 100 \cdot \frac{W_{wd} + W_{wsam}}{W_{dws}} \tag{15}$$

where W_{wsam} is the weight of water in the air dried soil sample, assumed to be 2% (WMO, 2008), W_{wd} is the weight of water added to achieve saturation and W_{dws} is the weight of the dry soil. The equation to determine EC_{sw} from EC_e is as follows:

$$EC_{sw} = f_{SP} EC_e \tag{16}$$

where:

$$f_{SP} = \theta_{SP}/\theta_{FC} \quad \text{for} \quad \theta \geqslant \theta_{FC} \tag{17}$$

$$f_{SP} = \theta_{SP}/\theta_{CR} \quad \text{for} \quad \theta_{FC} \geqslant \theta \geqslant \theta_{CR} \tag{18}$$

$$f_{SP} = \theta_{SP}/\theta_{PWP} \quad \text{for} \quad \theta < \theta_{CR} \tag{19}$$

2.1.3. Nutrient uptake

In the modified model, the uptake of dissolved Ca^{2+}, Mg^{2+} and Na^{+} is considered passive. Passive nutrient uptake is simulated by multiplying root water uptake with the dissolved nutrient concentration, for concentration values below a priori defined maximum concentration (C_{kmax}) (Šimůnek and Hopmans, 2009):

$$U_k(z,t) = S(h, h_o, z, t) min[C_k(z,t), C_{k\,max}] \tag{20}$$

where C_{kmax} (μg cm^{-3}) is the maximum concentration of the root uptake for the chemical species k. In this study, the maximum nutrient concentration for Ca^{2+}, Mg^{2+} and Na^{+} was calibrated with the measured values in the aboveground maize biomass.

2.2. Statistical analysis

The quantitative procedure of model evaluation was assessed using statistical analysis to calculate the average error (E), the root mean square error (*RMSE*) and the coefficient of residual mass (*CRM*) between the measured and computed values (Loague and Green, 1991; Antonopoulos, 2000). The statistical criteria are given by:

$$E = \sum_{i=1}^{n} \frac{P_i - O_i}{n} \tag{21}$$

$$RMSE = \left(\frac{1}{n-1}\sum_{i=1}^{n}(P_i - O_i)^2\right)^{1/2} \tag{22}$$

$$CRM = \left(\sum_{i=1}^{n} O_i - \sum_{i=1}^{n} P_i\right) \bigg/ \sum_{i=1}^{n} O_i \tag{23}$$

where O_i are the observed (measured) values, P_i are model predictions, and n is the number of observations. *RMSE* and *E* are given in the units of a particular variable, while *CRM* is dimensionless. Values of *E*, *RMSE*, and *CRM* close to zero indicate optimum model predictions. The *CRM* is a measure of the tendency of the model to overestimate or underestimate the measurements. A negative *CRM* shows a tendency to overestimate.

2.3. Experimental design and treatments

The study was conducted from 2009 to 2011 at the experimental farm of the Aristotle University of Thessaloniki (40°32N, 23°00E, 16 m above sea level) in Northern Greece, for three consecutive growing seasons of maize (April–October). The experiment was a split-plot design with three levels of EC_{iw} equal to 0.8, 3.2 and 6.4 dS m^{-1} and water amounts of 40 mm per irrigation, in two replicates. Treatments were AFI (EC_{iw} = 0.8 dS m^{-1}), CFI (EC_{iw} = 3.2 dS m^{-1}) and DFI (EC_{iw} = 6.4 dS m^{-1}). Treatment DFI was installed in 2010. During the experiment, full irrigation and deficit irrigation treatments with four levels of electrical conductivity were installed. Letter F stands for full irrigation treatments and letters A, B, C and D represent the level of electrical conductivity. The results of the deficit irrigation treatments and the treatment with EC_{iw} = 1.6 dS m^{-1} are not presented. Maize hybrid PR31G98 (FAO 700, Pioneer Hi-Breed Hellas) was sown in five rows, with plant rows 0.80 m apart and 0.16 m spacing between plants along the row. Fertilizer rates were similar to farming practice in the region. Nitrogen was applied at preplanting stage at 110 kg N ha^{-1}, as ammonium phosphate sulphate (22-11-0-13S).

The physical and initial chemical properties of the soil are given in Table 1. The soil profile was divided into four layers based on different physical soil properties. The soil layers were 0–15, 15–35, 35–90 and 90–110 cm.

Daily meteorological data were collected from a station nearby the experimental field. The data describe adequately the meteorological conditions of the Thessaloniki area, where the climate is considered typical of a semi-arid Mediterranean environment. Total annual rainfall was 416, 549 and 425 mm during the first, second and third year of the experiment, respectively. The reference evapotranspiration rate (ET_o) was calculated using the ASCE-standardized Penman–Monteith method (Allen et al., 2005).

Crop coefficients (K_c) for every treatment and year were estimated from measured leaf area index (*LAI*) values using the equations proposed by Kang et al. (2003) for maize. They were then adjusted for maize growth stages 30/40/50/30 days (Papazafiriou, 1996). Values for K_c ranged between K_{cini} = 0.37 ± 0.02, K_{cmid} = 1.36 ± 0.07 and K_{cend} = 0.21 ± 0.06. The crop evapotranspiration rate (ET_c) was calculated as the product of ET_o and K_c.

LAI was measured on a biweekly basis in each treatment during different stages of the maize cycle using the destructive-planimetric method, by measuring the area of all the leaves within a delimited area. The leaves of each sampled plant were scanned and the images were processed for the determination of the leaf area using the software Delta-T SCAN (Version 2.04nc; Delta-T Devices Ltd., Burwell, Cambridge, UK) (Aschonitis et al., 2014). The maximum values of LAI ranged between 5.85 ± 0.49 for AFI, 5.84 ± 0.26 for CFI and 5.89 ± 0.84 for DFI. Duplicate plant samples were taken at each sampling for the determination of LAI, dry weight and plant nutrient concentration.

Root depth was determined on a bi-weekly basis by observations of extracted root system until the middle of the cropping periods and measured root depth data were fitted to the logistic function using a maximum root depth of 75 cm as follows:

$$Rd_t = \frac{Rd_{max}}{1 + 58 \cdot exp\left[-8.85 \cdot \left(\frac{t}{t_{max}}\right)\right]} \tag{24}$$

where Rd_t is the root depth at day *t* and Rd_{max} is the maximum root depth at day t_{max}. A maximum root depth of 75 cm is characteristic of the hybrid and the conservative irrigation practice that was

Table 1
Initial physical and chemical soil properties.

Treatments	AFI				CFI				DFI			
Soil layer (cm)	0–35	35–75	75–90	90–110	0–35	35–75	75–90	90–110	0–35	35–75	75–90	90–110
Sand (%)	16	21	17	66	22	23	17	56	14	17	22	62
Silt (%)	51	56	48	24	44	52	55	29	54	58	49	26
Clay (%)	33	23	35	10	34	25	28	15	32	25	29	12
Texture	SiCL	SiL	SiCL	SL	CL	SiL	SiCL	SL	SiCL	SiL	CL	SL
Organic matter (%)	1.4	0.5	1.0	0.4	1.3	0.7	0.9	0.5	1.5	0.6	0.9	0.9
$CaCO_3$ (%)	9.5	5.2	4.7	3.7	8.5	4.0	3.7	2.8	9.0	4.7	4.8	4.7
EC_e (dS m^{-1})	0.79	1.02	1.42	3.22	0.99	1.64	3.98	4.72	0.68	0.94	1.53	2.61
Soluble ions (mmol$_{(c)}$ L^{-1})[a]												
Ca^{2+}	3.7	4.0	5.6	18.0	4.1	6.4	21.2	23.1	2.9	3.0	5.6	10.6
Mg^{2+}	2.3	3.7	5.2	12.6	3.2	6.7	20.0	23.6	1.8	3.0	5.1	9.3
Na^{+}	1.9	2.4	3.4	5.7	2.3	3.6	7.3	11.4	1.3	2.1	3.4	8.2
K^{+}	0.13	0.07	0.08	0.11	0.08	0.04	0.07	0.08	0.07	0.02	0.02	0.04
SAR ((mmol$_{(c)}$ L^{-1})$^{0.5}$)	1.097	1.223	1.463	1.457	1.204	1.407	1.608	2.359	0.848	1.212	1.470	2.600
Exchangeable cations (cmol$_{(c)}$ kg^{-1})												
Ca^{2+}	21.7	16.5	21.3	15.9	20.4	16.6	19.3	14.6	23.1	17.1	23.1	12.1
Mg^{2+}	7.0	7.3	11.0	8.1	7.3	9.6	11.6	7.5	7.6	9.1	12.7	5.1
Na^{+}	0.7	0.7	1.2	0.9	0.7	0.8	1.2	1.1	0.6	0.8	1.1	0.7
K^{+}	0.20	0.05	0.10	0.05	0.16	0.05	0.07	0.05	0.30	0.10	0.10	0.10
CEC (cmol$_{(c)}$ kg^{-1})[b]	29.6	24.5	33.6	25.0	28.6	27.1	32.2	23.2	31.6	27.0	36.9	18.0
ESP%	2.3	3.0	3.6	3.7	2.4	3.0	3.8	4.8	2.0	2.9	2.9	4.2

SiCL, Silty-Clay-Loam; SiL, Silty-Loam; SL, Sandy-Loam; CL, Clay Loam.
EC_e, electrical conductivity of the saturation paste extract.
SAR, sodium adsorption ratio; *CEC*, cation exchange capacity; *ESP%*, exchangeable sodium percentage.
[a] Measured in the saturation extract.
[b] Calculated from the sum of ion exchange species.

followed (Lekakis et al., 2011). The daily evolution of the root depth is provided as an input to model *WANISIM*.

Sowing date, fertilizer application date, duration of growing period, harvest date and cumulative ET_o during the three growing seasons are given in Table 2. Daily values of precipitation, irrigation and ET_o during the three years are presented in Fig. 1.

Irrigation water was applied uniformly on the soil surface using siphons. Water was pumped from reservoir tanks containing fresh water and the mixture of synthetic saline irrigation water. Treatments were separated by peripheral bunds after germination to prevent seepage, although no flooding conditions were observed in the field during irrigation. Irrigation water composition was obtained by adding different amounts of $CaCl_2$, NaCl and $MgCl_2$ to the water available in the region ($EC_{iw} \leqslant 1$ dS m^{-1}), maintaining a ratio of 3:3:2 for Ca^{2+}:Mg^{2+}:Na^{+} initially found in fresh water. In this study, NaCl was not used as the sole salinizing salt, because it is uncharacteristic of agriculturally saline environments, can cause adverse effects on soil physical properties and extreme ratios of Na/Ca, Na/K and Ca/Mg that can adversely affect the mineral-nutrient relations within the crop (Läuchli and Grattan, 2007). The balance between the cations was maintained the same, while concentrations were increased to obtain the desirable EC_{iw} of 3.2 and 6.4 dS m^{-1} for CFI and DFI treatments, respectively. The irrigation water salinity varied slightly from the average values that are reported within the same crop season and between crop seasons, according to small changes in the salinity of the locally available water used. Water composition was monitored in every irrigation event for concentrations of Ca^{2+}, Mg^{2+}, Na^{+} and levels of EC_{iw} during the three years. The average quality parameters of the applied irrigation water during the three years are presented in Table 3. According to the US Salinity Laboratory Staff (1954), irrigation water is characterized as highly saline water (C3) for AFI treatment and very highly saline water (C4) for CFI and DFI treatments and as low sodicity water (S1) for all the treatments. According to Ayers and Westcot (1985) irrigation water quality does not affect water infiltration, while it presents slight to moderate water availability effects for AFI and severe water availability effects for CFI and DFI treatments.

Six to eight irrigations at 7–10 days intervals were applied during the growing season. Irrigation amounts were conservative and scheduling was based on depletion of plant available water in the root zone. Irrigation was resumed when plant-available water was depleted to more than 50% of that achieved in last irrigation. The rainfall of the growing period was also taken into account in irrigation scheduling. Total irrigation amounts during the growing seasons of 2009, 2010 and 2011 were 260, 240 and 320 mm, respectively. The rainfall during the same period was 175, 185 and 99 mm, respectively for each growing season.

Soil moisture was measured with a dielectric profile probe PR2 (Delta-T Device Ltd). A site specific calibration of PR2 was performed in accordance to the instructions of the manufacturers (Profile Probe User Manual 2.0., Delta-T Device Ltd, 2004). The estimated parameters of the calibration equation were $a_0 = 1.47$ and $a_1 = 7.95$ ($r^2 = 0.902$). These calibrated values are in accordance with the findings of Kargas et al. (2011, 2012) and the default values given by the manufacturers. PR2 profile probe measures soil moisture vertically within ±5 cm of sensors located to the depths of 10, 20, 30, 40, 60 and 100 cm, thus corresponding to average soil moisture readings of 0–15, 15–25, 25–35, 35–45, 55–65 and 95–105 cm soil layers.

For the determination of the soil bulk density (ρ_b) and saturated volumetric water content (θ_s), undisturbed soil samples were collected at the beginning of the experiment from different soil layers. Cores of 5 cm height and 5 cm diameter were collected in thin-walled metal rings using sampling drill. The soil cores were wetted from below to saturation and the weights, before and after drying at 105 °C, were measured to determine the gravimetric saturated water content (Aschonitis et al., 2012). The bulk densities were measured at the same cores on dry weight.

The parameters a and n of the van Genuchten (1980) model and saturated hydraulic conductivity (K_{sat}), were estimated by inverse solution modeling, using HYDRUS-1D v4.0 (Šimůnek et al., 2008). Inverse modeling procedures are used increasingly to identify model parameters (Hopmans et al., 2002; Mertens et al., 2006). For the inverse solution, the measured soil water content at 10, 20, 30, 40, 60 and 100 cm soil depths of AFI treatment ($EC_{iw} = 0.8$ dS m^{-1}, without salinity stress), throughout the first year, were used to describe soil water movement in layers 0–15, 15–35, 35–90 and 90–110 cm. The parameters a, n and K_{sat} of the four layers were fitted simultaneously to the flow data. The θ_r was accepted as the initial estimation, according to the soil texture. The estimated soil water retention curve parameters were assumed to be the same for all treatments since the soil texture presented small differences between experimental plots. Table 4 lists the van Genuchten–Mualem parameters that describe the soil hydraulic functions of the soil layers in the experimental plots. The value of K_{sat} parameter for soil layer 90–110 cm was found very small and uncharacteristic of a coarse textured soil (Kutilek and Nielsen, 1994). This is attributed to a fifth layer consisted of a loamy, fine textured soil below 110 cm that affects the hydraulic conductivity of the overlying coarse textured layer.

The distribution coefficient, $K_{d,k}$ was measured as the ratio of the quantity of the cation adsorbed per unit mass of solid, A_i, to the quantity of the cation remaining in solution at equilibrium, C_i, as follows:

$$K_{d,k} = A_i / C_i \tag{25}$$

For the determination of $K_{d,k}$ values, the cations concentrations were measured in the solid and the liquid phase during the initial sampling. However, many solutes have been observed to sorb more readily than desorb from mineral or organic surfaces, a phenomena referred to as hysteresis (U.S.EPA, 1999). Therefore, the final values for $K_{d,k}$ were estimated by a trial and error procedure during model calibration. This procedure resulted in that less than 10% of the adsorbed Ca^{2+} and Mg^{2+} concentrations desorb, while for Na^{+}, this percentage was found higher, almost at 50%.

In the model, the hydrodynamic dispersion coefficient D is described by a simple functional relationship (Biggar and Nielsen, 1976) of the form:

$$D = D_o + \lambda v^n \tag{26}$$

where D_o (cm^2 h^{-1}) is the diffusion coefficient for a solute, v (cm h^{-1}) is the mean pore water velocity, λ (cm) is the dispersivity which is assumed to be a characteristic parameter of the medium structure and n is a coefficient. The values for λ and n were set equal to 0.122 cm and 1.11, respectively, according to Biggar and Nielsen

Table 2
Characteristics of the maize growing seasons.

Year	Fertilizer application	Sowing date	Germination date	Growing period duration	Harvest date	Cumulative ET_o (mm)
2009	6 April	29 April	7 May	140	15 September	709.5
2010	21 April	29 April	6 May	146	21 September	755.5
2011	20 May	20 May	26 May	139	4 October	716.7

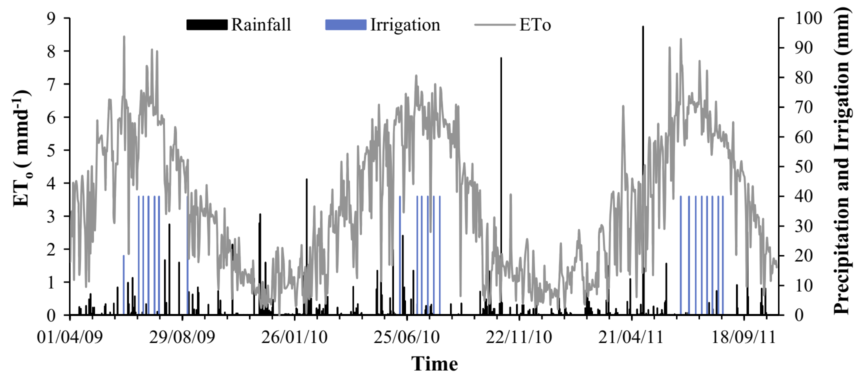

Fig. 1. Daily values of precipitation, irrigation and reference evapotranspiration rate (ET_o) from 1st April 2009 to 31st October 2011.

Table 3
Average ionic composition of irrigation water during the three years.

Year	Plot	EC_{iw} (dS m^{-1})	SAR	Soluble ions (mmol$_{(c)}$ L^{-1})		
				Ca^{2+}	Mg^{2+}	Na^+
2009	AFI	0.89	0.88	3.27	3.5	1.61
	CFI	3.36	2.46	10.39	13.87	8.57
2010	AFI	0.79	0.99	3.18	4.63	1.95
	CFI	3.17	1.98	13.18	17.8	7.8
	DFI	5.88	2.52	28.15	35.8	14.27
2011	AFI	0.87	0.81	2.28	3.4	1.35
	CFI	3.24	1.31	8.89	13.26	4.36
	DFI	6.01	1.63	17.74	24.97	7.55

Table 4
Parameters of the van Genuchten–Mualem soil hydraulic functions and solute transport parameters.

Parameter	Soil layer (cm)			
	0–15	15–35	35–90	90–110
θ_r (cm^3 cm^{-3})	0.089	0.089	0.067	0.065
θ_s (cm^3 cm^{-3})	0.520	0.592	0.592	0.499
α (cm^{-1})	0.031	0.004	0.014	0.002
n	1.314	1.307	1.228	2.679
K_s (cm h^{-1})	30.408	1.607	2.403	0.015
ρ_b (g cm^{-3})	1.450	1.450	1.140	1.630
D_o (cm^2 h^{-1})	0.0324	0.0324	0.0205	0.0353
λ (cm)	0.122	0.122	0.122	0.122
K_d (cm^3 g^{-1})				
Ca^{2+}	0.24	0.24	0.33	0.23
Mg^{2+}	0.21	0.21	0.25	0.24
Na^+	1.10	1.10	0.45	0.40
K^+	0.30	0.30	0.42	0.26

(1976) and D_o was also derived from the literature (Rowe and Badv, 1996; Tinker and Nye, 2000). The $K_{d,k}$ and D_o coefficients of the soil layers are presented in Table 4.

The concentrations of soluble cations Ca^{2+}, Mg^{2+}, Na^+ and electrical conductivity (EC_e) were monitored in the saturation extracts of the soil layers 0–35 and 35–75 cm during the growing periods. Soil samples were collected generally 24 h before an irrigation event from each treatment and replication. The concentrations of Ca^{2+}, Mg^{2+} and Na^+ in the saturation extract and irrigation water were determined using ICP according to APHA (2005). Soil EC_e was measured according to Rhoades (1996). Organic matter was determined with the wet oxidation method of Walkley and Black (1934) and calcium carbonate ($CaCO_3$) with the volumetric calcimeter method (Allison and Moodie, 1965). Particle size analysis was performed with the hydrometer method (Bouyoucos, 1962). Exchangeable cations Mg^{2+}, Ca^{2+} and Na^+ were extracted with the ammonium acetate method at pH 8.2 (Thomas, 1982) and determined using ICP. Concentrations of Mg^{2+}, Ca^{2+} and Na^+ in the aboveground biomass were determined after destruction of the organic matter with the dry ashing method and measured in ICP following the procedure described by Donohue and Aho (1992).

2.4. Model parameterization

Simulations of soil water content, concentrations of individual cations (Na^+, Ca^{2+} and Mg^{2+}) and overall salinity, were performed with the model *WANISIM* for the growing and the rainfall-winter periods of the years 2009, 2010 and 2011. The simulated soil profile depth was 110 cm and the discretization along the z-axis was 2.5 cm. The time step varied from 0.001 to 0.01 days. The moisture change during one time step was kept lower than 0.001 cm^3 cm^{-3}. The surface boundary condition was defined as known flux (Neumann condition), equal to the net rainfall plus irrigation minus soil evaporation for soil water, and as known mass load for individual ions, multiplying the concentration by the rate of irrigation water. The bottom boundary condition was defined as free drainage.

Cations concentrations were measured at every irrigation event, at each plot, in irrigation water samples. These concentrations were used as specific model input for every irrigation event. The initial soil water content and concentrations of Na^+, Ca^{2+} and Mg^{2+} were provided as input, based on the initial measured volumetric soil moisture and solute concentrations of Table 1. The parameters calibrated with experimental data from the years 2009 and 2010 and validated with data from 2011, were the distribution-partition coefficients, $K_{d,k}$, and the parameter of the maximum passive nutrient uptake, C_{kmax}, for Ca^{2+}, Mg^{2+} and Na^+.

In the model, the electrical conductivity of the threshold-slope model of Homaee et al. (2002) is converted from EC_e to EC_{sw} using the f_{SP} ratios, depending on the moisture of the soil layer. The slope is divided by the same ratio. The ratios were also used to adjust the initial input ion concentrations measured in the saturation extract to the initial soil moisture and for comparison purposes between measured and computed values. The f_{SP} ratios ranged from 1.3 to 2.1 in soil layer 0–35 cm, from 1.5 to 2.6 in soil layer 35–75 cm, from 1.7 to 3.0 in soil layer 75–95 cm and from 1.0 to 4.0 in soil layer 90–110 cm.

3. Results and discussion

3.1. Volumetric water contents

Figs. 2–4 present the computed and measured soil water contents for treatments AFI, CFI and DFI. The statistical criteria E,

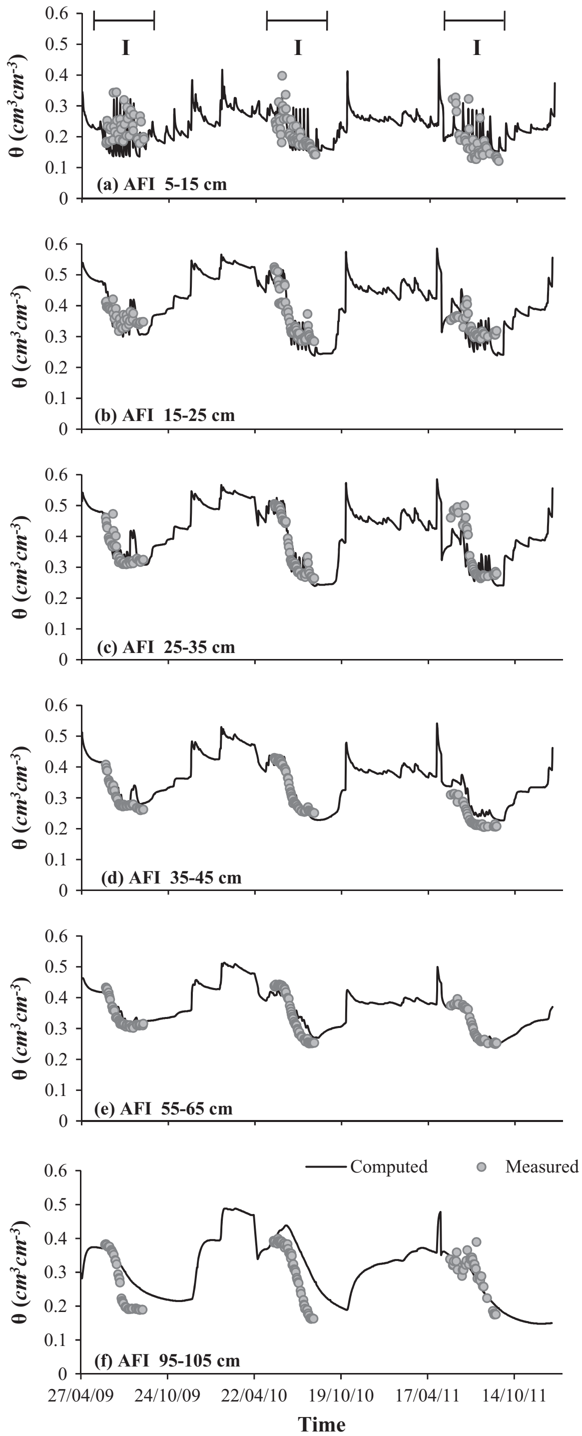

Fig. 2. Measured and computed volumetric water contents at 0–15, 15–25, 25–35, 35–45, 55–65 and 95–105 cm layers in treatment AFI, during the simulation period (28/4/2009–31/12/2011). Symbol I denotes the irrigation periods.

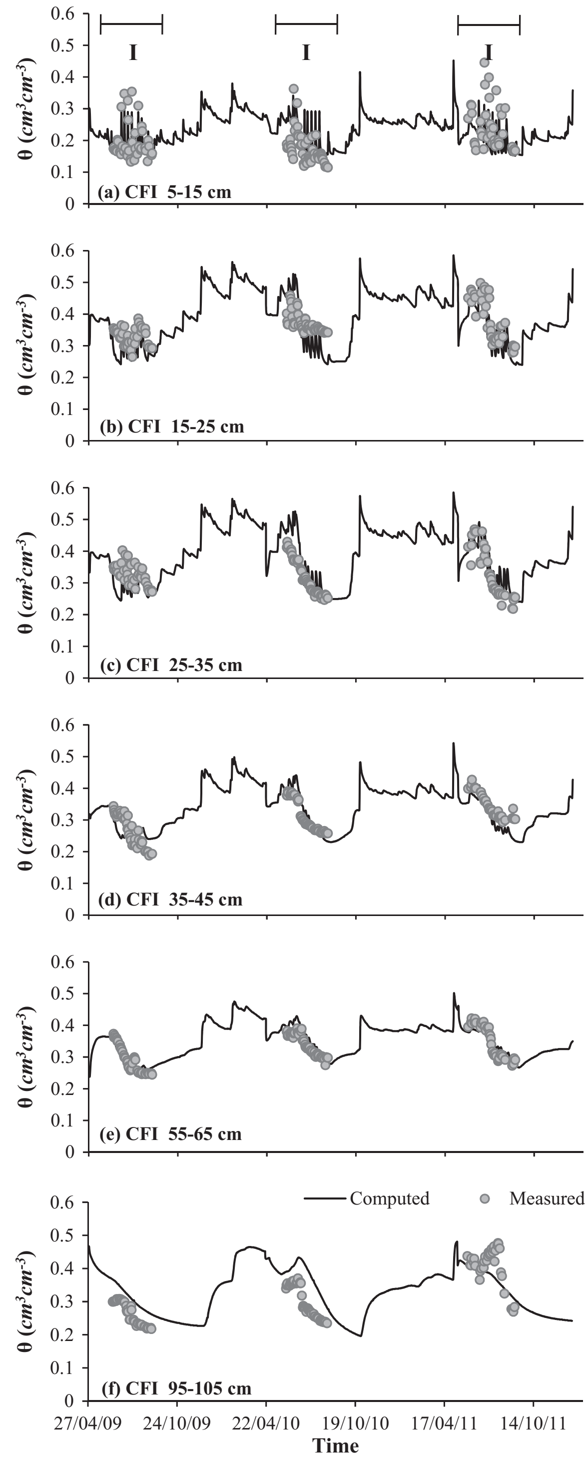

Fig. 3. Measured and computed volumetric water contents at 0–15, 15–25, 25–35, 35–45, 55–65 and 95–105 cm layers in treatment CFI, during the simulation period (28/4/2009–31/12/2011). Symbol I denotes the irrigation periods.

RMSE and *CRM* between computed and measured soil moisture, during calibration and validation, are summarized in Table 5.

The discrepancy between the measured and simulated water content is generally small. The average error (*E*) ranged from $-0.017\ cm^3\ cm^{-3}$ to $0.028\ cm^3\ cm^{-3}$ and the root mean square error (*RMSE*) ranged from $0.04\ cm^3\ cm^{-3}$ to $0.06\ cm^3\ cm^{-3}$ during calibration and validation. The coefficient of residual mass (*CRM*) values indicate that the model overestimates soil moisture (−0.04 to −0.03) during calibration, while it underestimates soil moisture of AFI and CFI treatments (0.0–0.05) and overestimates that of DFI treatment (−0.09), during validation.

The overall performance of the soil moisture simulation is evaluated by comparing the statistical criteria with those obtained in previous studies, using different models for the description of soil water dynamics. Bonfante et al. (2010) compared the performance of SWAP, CropSyst and MACRO models and obtained *RMSE* values ranging from 0.01 to $0.08\ cm^3\ cm^{-3}$ for different soils and

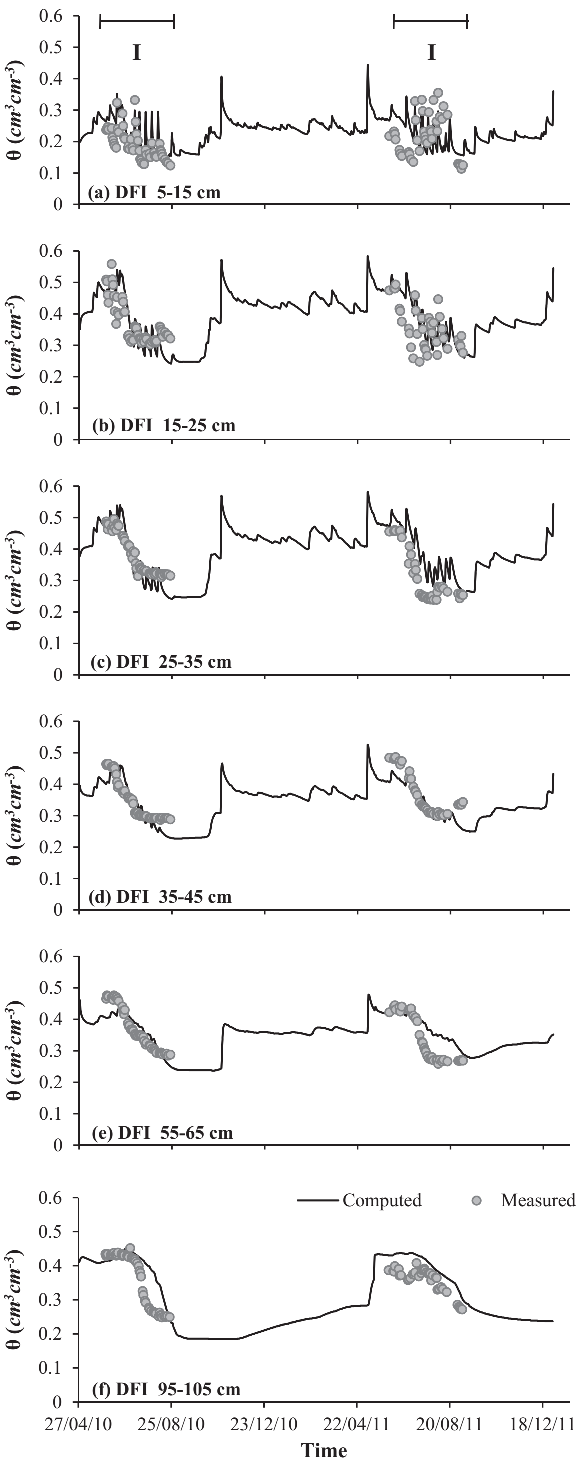

Fig. 4. Measured and computed volumetric water contents at 0–15, 15–25, 25–35, 35–45, 55–65 and 95–105 cm layers in treatment DFI, during the simulation period (28/4/2009–31/12/2011). Symbol I denotes the irrigation periods.

models. Antonopoulos (2000) using *WANISIM* model, direct measurements and pedotransfer functions for the determination of the soil hydraulic properties in a corn field, obtained *RMSE* values ranging from 0.03 to 0.10 $cm^3\ cm^{-3}$. Jarvis et al. (2000) using MACRO model, considered acceptable the simulations of soil water content with average values of *RMSE* less than 0.06 $cm^3\ cm^{-3}$ and absolute values of *CRM* less than 0.07.

Soil moisture fluctuation followed the wetting and drying cycles in the 0–15 cm soil layer, reaching values close to field capacity immediately after an irrigation event and decreasing rapidly due to the effects of high evapotranspiration rates, during the growing periods. Water simulation results present almost the same fluctuation at the 15–25 and 25–35 cm soil layers following to a lesser extent the wet and dry cycles of the irrigation events in all three treatments. Although the initial soil moisture was between field capacity and saturation, it was soon depleted and remained low due to water uptake by plant roots. Soil water distributions at the 35–45 and 55–65 cm layers show smaller water content variations caused by the applied irrigation water. Soil moisture was reduced dramatically as soon as roots reached the depth of 55 cm in all three treatments. Soil moisture was also depleted from the layer 95–105 cm during the growing seasons. Since this layer lies outside of the root zone, decreasing moisture is attributed to capillary rise of water due to increased evapotranspiration rates in the overlying soil layers. Furthermore, the computed soil water balance in the treatments showed limited deep percolation, thus justifying upward movement of water. Specifically, during the growing and non growing seasons, results show less than 10 mm totally percolated water under the 110 cm soil profile for AFI, zero percolation for CFI and less than 1 mm total deep percolation for DFI.

It must be noted that the total irrigation amount applied per growing season is not considered sufficient for corn, according to the usual practice in the area (Georgiou et al., 2010; Dioudis et al., 2009). The range of cumulative ET_c during the growing seasons was 545 ± 33 mm for AFI, 535 ± 16 mm for CFI and 563 mm for DFI. Considering that the amounts of irrigation and rainfall were 435, 425 and 419 mm for 2009, 2010 and 2011, respectively, crop evapotranspiration demands were not met and the irrigation amount could be characterized as conservative. This is reflected in the measured and simulated soil moisture distribution. A small amount of water is infiltrated to the soil layers of 15–25 and 25–35 cm but it is soon depleted and remains low due to excess water uptake by plant roots. Furthermore, soil moisture is reduced dramatically as soon as roots reach the depth of 55 cm in all three treatments and moisture decreasing in soil layer 95–105 cm can only be attributed to upward movement of water due to the hydraulic gradient.

3.2. Water balance components and root water uptake

The computed cumulative water balance components (irrigation and rainfall, potential and actual transpiration and evaporation) for every growing season, considering either only water stress or both water and osmotic stress, are listed in Table 6. The cumulative amount of water applied during the three growing periods was 1260 mm of which 435 mm was rainfall. Simulations were carried out with *WANISIM* model considering or not the effect of the osmotic stress on the water uptake (transpiration). Under water stress only, actual transpiration and evaporation during the growing periods were 1486 mm and 164 mm, respectively, in AFI treatment, 1483 mm and 117 mm, respectively, in CFI treatment (2009–2011), 1023 mm and 108 mm, respectively, in DFI treatment (2010 and 2011). Due to water stress, transpiration in AFI decreased a total of 312 mm, in CFI 307 mm and in DFI 166 mm. Under combined water and osmotic stress, root water uptake was further reduced in all plots either irrigated with fresh or saline water, by less than 2 mm in AFI, 11 mm in CFI and approximately 4 mm in DFI. Treatments present similar transpiration because corn hybrid PR31G98 develops significant above ground biomass as it is intended both for silage and grain production and the development was further promoted by the rainfalls of May and June at the early growth stages, until the middle of the growing seasons.

Table 5
Statistical analysis between measured and computed soil water content (obtained for the studied depths of 5–15, 15–25, 25–35, 55–65, 95–105 cm), Ca^{2+}, Mg^{2+} and Na^{+} concentration, EC_{sw} and *SAR* (obtained for the studied depths of 0–35 and 35–75 cm) during the calibration and validation procedure.

Treatment	2009–2010			2011		
	E	*RMSE*	*CRM*	*E*	*RMSE*	*CRM*
Soil moisture content						
	($cm^3\ cm^{-3}$)	($cm^3\ cm^{-3}$)	(–)	($cm^3\ cm^{-3}$)	($cm^3\ cm^{-3}$)	(–)
AFI	0.012	0.05	−0.04	−0.001	0.04	0.00
CFI	0.012	0.05	−0.04	−0.017	0.05	0.05
DFI	0.012	0.05	−0.03	0.028	0.06	−0.09
Concentration of Ca^{2+} in the soil solution						
	($mmol_{(c)}\ L^{-1}$)	($mmol_{(c)}\ L^{-1}$)	(–)	($mmol_{(c)}\ L^{-1}$)	($mmol_{(c)}\ L^{-1}$)	(–)
AFI	−0.065	2.96	0.01	1.017	2.38	−0.10
CFI	1.019	3.60	−0.06	−1.657	4.55	0.06
DFI	−7.948	12.65	0.37	−7.070	13.10	0.19
Concentration of Mg^{2+} in the soil solution						
AFI	−0.817	2.43	0.12	1.085	2.87	−0.25
CFI	2.960	6.41	−0.18	0.649	5.64	−0.03
DFI	−1.208	7.25	0.08	11.832	14.92	−0.46
Concentration of Na^{+} in the soil solution						
AFI	0.124	1.07	−0.03	−0.264	1.06	0.07
CFI	−0.361	2.57	0.04	0.280	1.89	−0.02
DFI	0.111	2.26	−0.02	−2.369	3.98	0.24
EC_{sw}						
	($dS\ m^{-1}$)	($dS\ m^{-1}$)	(–)	($dS\ m^{-1}$)	($dS\ m^{-1}$)	(–)
AFI	−0.242	0.65	0.12	0.049	0.48	−0.02
CFI	0.033	0.96	−0.01	−0.826	1.22	0.12
DFI	−1.614	2.81	0.32	−0.319	1.56	0.04
SAR of the soil solution						
	($mmol_{(c)}\ L^{-1})^{0.5}$	($mmol_{(c)}\ L^{-1})^{0.5}$	(–)	($mmol_{(c)}\ L^{-1})^{0.5}$	($mmol_{(c)}\ L^{-1})^{0.5}$	(–)
AFI	0.106	0.30	−0.08	−0.191	0.34	0.15
CFI	−0.172	0.57	0.08	0.096	0.34	−0.04
DFI	0.362	0.62	−0.30	−0.431	0.67	0.25

Table 6
Components of soil water balance at the end of each growing period for the three treatments (Irr. & Rain: Irrigation and Rainfall, Pot. Trans.: Potential Transpiration, Act. Trans.: Actual Transpiration, Act. Evap.: Actual Evaporation).

Water balance (mm)		2009		2010		2011	
		No osmotic stress	Osmotic stress	No osmotic stress	Osmotic stress	No osmotic stress	Osmotic stress
AFI	Irr. & Rain	434.76	434.76	425.41	425.41	419.01	419.01
	Pot. Trans.	548.53	548.53	642.43	642.43	607.43	607.43
	Act. Trans.	494.55	494.34	523.34	523.19	468.14	467.05
	Act. Evap.	63.57	63.59	55.20	55.19	44.75	44.75
CFI	Pot. Trans.	608.40	608.40	599.70	599.70	581.92	581.92
	Act. Trans.	490.32	488.78	506.39	502.82	486.22	480.25
	Act. Evap.	30.02	30.04	48.41	48.47	38.06	38.08
DFI	Pot. Trans.			649.96	649.96	537.53	537.53
	Act. Trans.			522.39	521.70	499.42	496.60
	Act. Evap.			41.50	41.79	66.18	66.81

Water uptake was reduced due to osmotic stress in AFI treatment mainly in 2011, by 1.1 mm, because of the composition of the fresh water that led to a computed EC_{sw} which marginally exceeded the calculated threshold for corn of the Maas and Hoffman (1977) model, during the irrigation period. In treatment CFI which was irrigated with saline water (EC_{iw} = 3.2 dS m^{-1}) the reduction due to osmotic stress was 1.5 mm in 2009, 3.6 mm in 2010 and 6.0 mm in 2011, as EC_{sw} reached very high values and became three times greater than the threshold electrical conductivity during the irrigation periods. In treatment DFI, which was irrigated with saline water (EC_{iw} = 6.4 dS m^{-1}) osmotic stress reduced water uptake by 0.7 mm in 2010 and 2.8 mm in 2011. Despite the fact that DFI treatment was irrigated with waters of the highest EC_{iw}, the osmotic stress effects on the cumulative root water uptake were relatively minor in comparison to CFI treatment. This phenomenon can be justified by the low initial salt concentrations in the soil profile of treatment DFI compared to CFI.

Ramos et al. (2011) used model UNSATCHEM to calculate reductions in root water uptake of maize in a field experiment and reported reductions as high as 866 mm due to water stress and 276 mm due to osmotic stress for three consecutive growing periods, using blended saline irrigation waters of EC_{iw} = 8 dS m^{-1}. The researchers followed an irrigation scheduling were water was applied in order to maintain soil water content between saturation and field capacity. Gonçalves et al. (2006) using HYDRUS-1D predicted 910 mm reductions in transpiration due to water stress and 120 mm reductions due to osmotic stress in a four year experiment in lysimeters, covered by annual spontaneous vegetation in which saline irrigation water of EC_{iw} = 3.2 dS m^{-1} was used. These researchers also maintained the soil moisture to the level of field capacity during the irrigation periods. In the present study, irrigation was applied almost weekly with 6–7 day intervals, exposing plants to periods of dry conditions, possibly increasing plant salt tolerance and maintaining low rates of water uptake between irrigations. Shani and Dudley (2001) found that plant salt tolerance increases during periods of time when the region near the root is severely moisture depleted and the hydraulic conductivity is sufficiently low to create a flux-limited condition, thus minimizing the effect of the osmotic potential on crop-water relations. The previous is interpreted in *WANISIM* model by multiplying the threshold salinity of the Maas and Hoffman (1977) model with the appropriate f_{SP} ratio, according to the soil moisture. The ratio is higher in low moisture levels and the threshold salinity increases, increasing plant salt tolerance in drier conditions. Indeed, model results reveal that water uptake continued in small amounts between irrigations in deeper than 15 cm soil layers for treatments CFI and DFI, compensating in this way the reductions in water uptake due to osmotic stress.

3.3. Individual Ions

Measured and simulated concentrations of Ca^{2+}, Mg^{2+} and Na^{+} for treatments AFI, CFI and DFI, are presented in Figs. 5–7, respectively. The statistical criteria *E*, *RMSE* and *CRM* during calibration and validation for Ca^{2+}, Mg^{2+} and Na^{+} are summarized in Table 5. For the determination of the ions concentration in the soil solution, measured concentrations were multiplied with the ratio f_{SP} according to the water content of the soil layer at the particular day of measurement. These values were then compared with computed concentration values.

Predicted values for Ca^{2+}, Mg^{2+} and Na^{+} concentrations during calibration and validation were in a generally good agreement with the measured values for AFI and CFI treatments, while less satisfactory for DFI treatment. *RMSE* calculated for Ca^{2+} concentrations resulted in values less than 4.55 $mmol_{(c)}\,L^{-1}$ for AFI and CFI, while as high as 13.10 $mmol_{(c)}\,L^{-1}$ for DFI. *RMSE* values obtained for Mg^{2+} were lower than 6.41 $mmol_{(c)}\,L^{-1}$ for AFI and CFI and lower than 14.92 $mmol_{(c)}\,L^{-1}$ for DFI treatment. *RMSE* values obtained for Na^{+} during the calibration and validation years were lower than 3.98 $mmol_{(c)}\,L^{-1}$ in all treatments at both soil layers. *CRM* reveals a general underestimation of Ca^{2+}, overestimation of Mg^{2+} and not a clear trend for Na^{+} values.

Ramos et al. (2011) used HYDRUS-1D model for the simulation of major cations in a field experiment and obtained *RMSE* values between measured and predicted Ca^{2+}, Mg^{2+} and Na^{+} concentrations, as high as 5.66, 4.16 and 13.86 $mmol_{(c)}\,L^{-1}$, respectively.

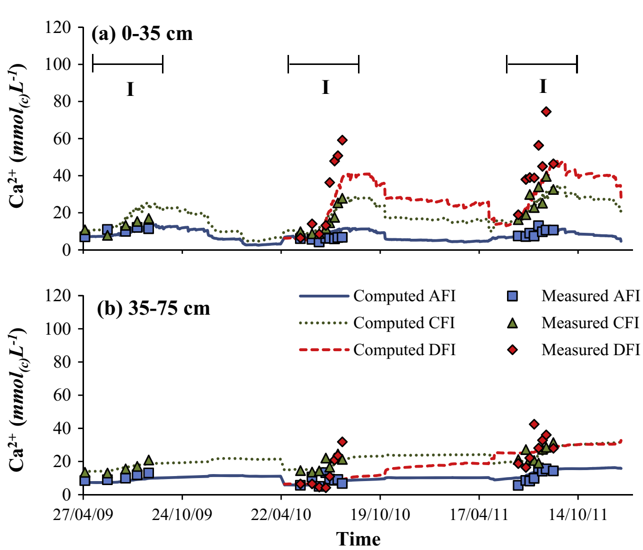

Fig. 5. Measured and computed Ca^{2+} concentrations of the soil solution at 0–35 and 35–75 cm soil layers in the three treatments, during the growing seasons and subsequent rainfall periods. Symbol I denotes the irrigation periods.

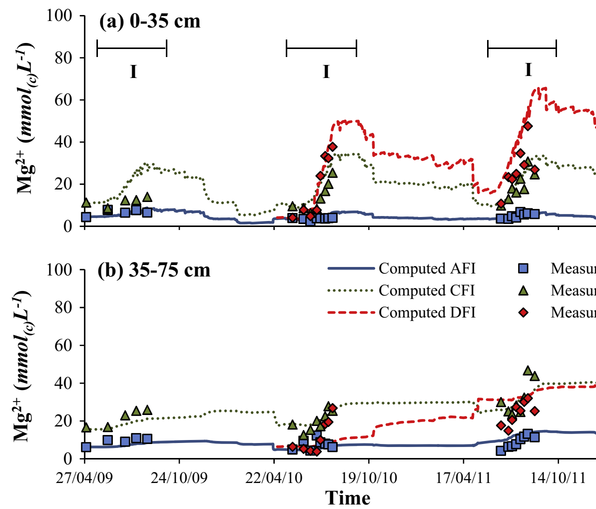

Fig. 6. Measured and computed Mg^{2+} concentrations of the soil solution at 0–35 and 35–75 cm soil layers in the three treatments, during the growing seasons and subsequent rainfall periods. Symbol I denotes the irrigation periods.

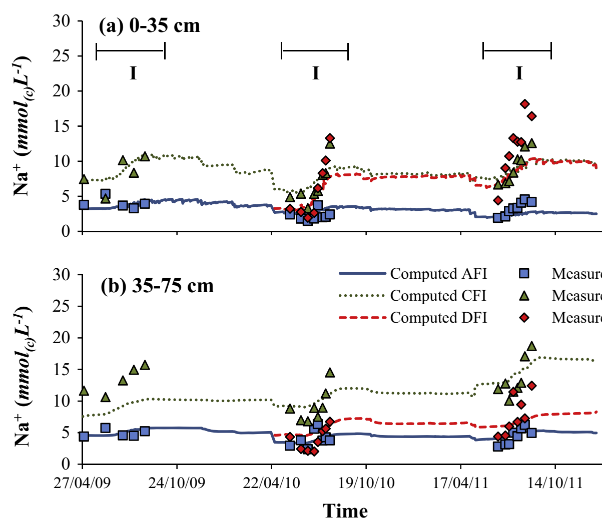

Fig. 7. Measured and computed Na^{+} concentrations of the soil solution at 0–35 and 35–75 cm soil layers in the three treatments, during the growing seasons and subsequent rainfall periods. Symbol I denotes the irrigation periods.

The researchers used an average ionic composition of irrigation water consisting of 1.95, 2.18 and 80.00 $mmol_{(c)}\,L^{-1}$, Ca^{2+}, Mg^{2+} and Na^{+}, respectively. Yurtseven et al. (2013) also used HYDRUS-1D model, in a study with different water salinity levels in soil columns sown with alfalfa, and obtained *RMSE* values for Ca^{2+}, Mg^{2+} and Na^{+} concentrations as high as 16.20, 9.94 and 14.97 $mmol_{(c)}\,L^{-1}$, respectively. The average ionic composition of their irrigation water was 13.53, 0.76 and 1.98 $mmol_{(c)}\,L^{-1}$, Ca^{2+}, Mg^{2+} and Na^{+}, respectively. In this study the average ionic composition of the irrigation waters for CFI and DFI treatments, was 15.67, 21.14 and 8.51 $mmol_{(c)}\,L^{-1}$, Ca^{2+}, Mg^{2+} and Na^{+}, respectively. The comparison with other studies reveals that, although *WANISIM* does not account for equilibrium chemical reactions between major ions, it predicts successfully the major cations transport in the 0–35 and 35–75 cm soil layers.

In general, peak values of Ca^{2+} concentration in the treatments were observed in late August–early September periods and the highest values during 2011. The higher Ca^{2+} concentration values in CFI and DFI were more than double the concentration of the saline irrigation waters. Calcium concentrations subsequently decreased during the rainfall periods in the surface layer, reaching values similar to the initial conditions after the first irrigation season but higher than the initial conditions after the second irrigation season for all treatments.

The dynamics of Mg^{2+} were similar to those of Ca^{2+} throughout the simulation period in both soil layers. The highest value of Mg^{2+} in the upper soil layer was observed in DFI treatment after the third irrigation period. The concentration of Mg^{2+} gradually increased in the deeper soil layer for DFI and CFI treatments after the first irrigation season. The increase in Mg^{2+} and Ca^{2+} concentration in the 35–75 cm soil layer in DFI is not analogous to the irrigation water composition, compared to CFI. This is due to the higher initial salt concentration of CFI. Nevertheless, the use of the irrigation water with $EC_{sw} = 6.4\ dS\ m^{-1}$ led to high values for calcium and magnesium in the deeper layer of treatment DFI, similar to CFI, within only two irrigation cycles.

Smaller but noticeable increase in sodium concentration was observed and computed by *WANISIM*, as it was the cation with the lowest concentration being added to the saline irrigation waters. In the upper layer of the treatments DFI and CFI, Na^{+} increased after the irrigation periods in almost the same levels, while it was maintained almost constant in AFI throughout the simulation period.

The mass balance components for Ca^{2+}, Mg^{2+} and Na^{+} during the simulation period are presented in Table 7. According to the results, significant amounts of the ions were added in the soil through the irrigation water, in treatments CFI and DFI. Computed leaching losses were limited, as was deep percolation, and mainly observed after the first irrigation season for treatment AFI and after the second irrigation season for treatment DFI. No leaching was computed for treatment CFI during the simulation period. This can be attributed to three main reasons: (i) the conservative irrigation water amount, (ii) the fast depletion of soil moisture in the rhizosphere due to increased evapotranspiration during the summer months, which inhibits water movement to deeper layers and (iii) the upward movement of water, initially stored at 95–105 cm soil layer, because of soil moisture depletion in the upper soil layers. Therefore, high quantities of the applied salts remained in the soil profile of 110 cm. The calculated mass balance errors of the ions transport simulation were very low.

Table 7
Ca^{2+}, Mg^{2+} and Na^{+} mass balance for the three treatments during the simulation period.

Mass balance components (kg ha^{-1})	Ca^{2+}	Mg^{2+}	Na^{+}
AFI 2009–2011			
Initial mass in the liquid phase	1276.1	715.8	734.2
Initial mass in the solid phase	1166.4	613.9	1301.4
Inflow – irrigation load	457.5	378.9	299.7
Plant uptake	262.5	300.5	56.8
Leaching	76.0	47.5	39.2
Final mass in the liquid phase	1521.8	760.7	991.3
Final mass in the solid phase	1039.7	599.9	1248.0
Mass stored in the soil profile	119.0	30.9	203.7
CFI 2009–2011			
Initial mass in the liquid phase	1402.7	864.5	872.5
Initial mass in the solid phase	1228.4	683.1	1844
Inflow – irrigation load	1745.0	1469.1	1234.8
Plant uptake	247.7	286.3	52
Leaching	0.0	0.0	0.0
Final mass in the liquid phase	2325.4	1530.6	1533.1
Final mass in the solid phase	1802.9	1199.8	2366
Mass stored in the soil profile	1497.2	1182.8	1182.7
DFI 2010–2011			
Initial mass in the liquid phase	1281.9	647.7	869.4
Initial mass in the solid phase	1067.2	481.3	1392.0
Inflow – irrigation load	2513.6	2041.4	1352.0
Plant uptake	183.2	211.6	38.2
Leaching	8.0	4.0	6.0
Final mass in the liquid phase	2522.3	1623.0	1220.2
Final mass in the solid phase	2149.2	1331.9	2349.0
Mass stored in the soil profile	2322.4	1825.8	1307.8

3.4. Overall salinity and sodicity

The average measured and computed EC_{sw} are illustrated in Fig. 8. The statistical criteria during calibration and validation, concerning measured and predicted EC_{sw}, are summarized in Table 5. *WANISIM* simulations of the total soil salinity resulted in a generally good agreement with the observed distributions in all of the three treatments throughout the simulation period. Average *RMSE* resulted in values lower than 0.65, 1.22 and 2.81 $dS\ m^{-1}$ for the treatments AFI, CFI and DFI respectively, indicating relatively good overall correspondence between measured and simulated data. In general, positive *CRM* values indicate an underestimation of the measured EC_{sw}.

Soil salinity increased considerably in treatments irrigated with saline waters. In CFI, computed and measured soil salinity reached maximum values during the last irrigation season. During the rainfall periods, soil salinity decreased in the surface layer and increased in the deeper layer, due to salt leaching. In CFI, salts began to build up at the layer of 0–35 cm after the second irrigation season and at the layer of 35–75 cm after the first irrigation season, as rainfall was not sufficient to remove salts below the root zone.

In treatment DFI, computed and measured EC_{sw} of the surface soil layer, increased significantly, from approximately 2 $dS\ m^{-1}$ to values higher than 12 $dS\ m^{-1}$, during the last irrigation season. A large amount of rainwater (97 mm), in early May of 2011, leached salts from the top layer and lowered EC_{sw} until the irrigation period of 2011. In layer 35–75 cm, soil salinity increased continuously during 2010 and 2011 as a result of salt leaching from the surface layer.

The use of the locally available water did not lead to soil salinization, although salt leaching from the surface soil layer caused an increase in the EC_{sw} of the 35–75 cm layer to marginally saline levels of 4 $dS\ m^{-1}$. Saline irrigation water of $EC_{iw} = 3.2\ dS\ m^{-1}$ caused soil salinization after the first irrigation period in both soil layers. The use of saline irrigation water with $EC_{iw} = 6.4\ dS\ m^{-1}$ had the biggest effect on the soil solution salinity within only two

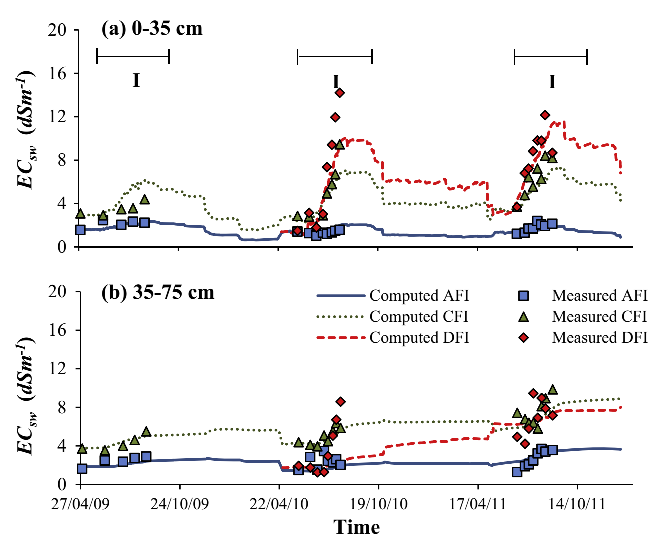

Fig. 8. Measured and computed soil solution electrical conductivities, EC_{sw}, at 0–35 and 35–75 cm soil layers in the three treatments, during the growing seasons and subsequent rainfall periods. Symbol I denotes the irrigation periods.

irrigation periods. The increase in the salinity of the 35–75 cm soil layer in all three treatments is mainly attributed to the limited percolation and leaching of salts below the root zone and the 110 cm soil profile, as predicted by the model results. It is evident that the general behavior of EC_{sw} is the same as that of calcium because it is the most important contributor to EC_{sw} considering the composition of the fresh and saline irrigation waters.

The average measured and computed *SAR* of the soil solution are illustrated in Fig. 9. The statistical criteria *E*, *RMSE* and *CRM* during calibration and validation concerning measured and predicted *SAR* are summarized in Table 5. Average *RMSE* values for both soil layers, lower that 0.62 $(mmol_{(c)}\,L^{-1})^{0.5}$ for the calibration years and lower that 0.67 $(mmol_{(c)}\,L^{-1})^{0.5}$ for the validation year in all three treatments, show that the model is able to predict soil *SAR* with an acceptable accuracy.

In AFI treatment, computed *SAR* values remained almost the same during the three growing periods at both soil layers. CFI presented the highest initial soluble Na^{+} and *SAR* values compared to the other treatments in both soil layers. However, the composition of the saline irrigation waters used, maintained *SAR* approximately at 2.2 $(mmol_{(c)}\,L^{-1})^{0.5}$ throughout the growing periods in both soil layers. The same fluctuation was observed in computed *SAR* values of treatment DFI, where average *SAR* was 1.5 $(mmol_{(c)}\,L^{-1})^{0.5}$ at soil layers 0–35 and 35–75 cm. During the winter season of 2010, an increase in soil *SAR* is observed at the 0–35 cm soil layer in treatments AFI and DFI, which is attributed to significant leaching of Ca^{2+} and Mg^{2+} from the surface layer and continuous desorption of exchangeable Na^{+}.

Rasouli et al. (2013) used model UNSATCHEM to predict EC_{sw} in a field experiment with winter wheat and varying irrigation water salinities. They obtained *RMSE* values that ranged from 0.52 to 1.01 dS m^{-1} and from 1.60 to 2.13 dS m^{-1} for the validation period, with irrigation water salinities of 6.5 and 11.5 dS m^{-1}, respectively. Ramos et al. (2011) calculated *RMSE* values for EC_{sw} as high as 2.35 dS m^{-1} using HYDRUS-1D and 2.04 dS m^{-1} using UNSATCHEM, with an average irrigation water salinity of 8.9 dS m^{-1}. The researchers also obtained *RMSE* values for predicted *SAR* as high as 6.27 $(mmol_{(c)}\,L^{-1})^{0.5}$.

SAR is a variable that characterizes salt affected soils and takes into consideration that the adverse effects of sodium are moderated by the presence of calcium and magnesium ions (Gonçalves et al., 2006). The use of saline irrigation waters in treatments CFI and DFI with a ratio of 3:3:2 for Ca^{2+}:Mg^{2+}:Na^{+}, with $SAR < 2.52$ $(mmol_{(c)}\,L^{-1})^{0.5}$ and $EC_{iw} > 3.17$ dS m^{-1} do not pose a soil sodification threat and eventually water infiltration problems. Soil *SAR* values greater than 13 $(mmol_{(c)}\,L^{-1})^{0.5}$ indicate a sodic soil (US Salinity Laboratory Staff, 1954). However, in this study, measured and computed high concentrations of Ca^{2+} and Mg^{2+} compared to Na^{+} in the irrigation water and the soil solution, did not lead to soil sodification, thus maintaining *SAR* values below 4 $(mmol_{(c)}\,L^{-1})^{0.5}$ in all treatments, during the three year experiment.

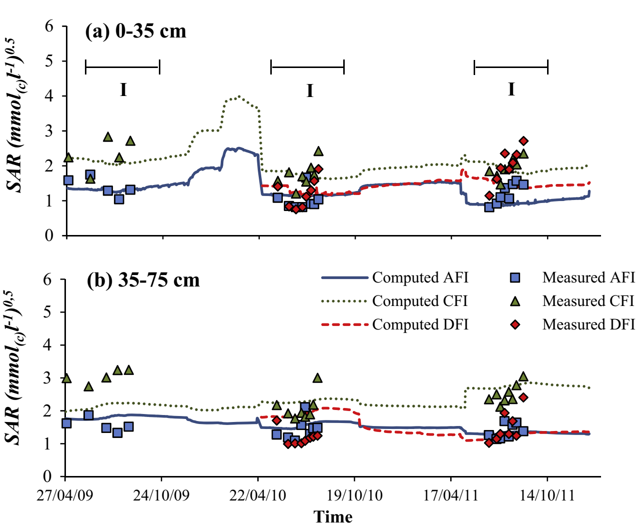

Fig. 9. Measured and computed soil *SAR* at 0–35 and 35–75 cm soil layers in the three treatments, during the growing seasons and subsequent rainfall periods. Symbol I denotes the irrigation periods.

3.5. Cations uptake

Following the approach of Šimůnek and Hopmans (2009), passive nutrient uptake is described in model *WANISIM* by multiplying root water uptake with the dissolved nutrient concentration, for soil solution concentration values below C_{kmax}. Uptake was considered to last until harvest because accumulation of macronutrients in maize continues throughout the growing season with most of the nutrients being absorbed between anthesis and ripening (Fageria, 2009). It is specifically noted that the C_{kmax} approach does not take into account the abundance of cations in the soil solution, nor the interactions between cations due to changes in the ratios of Na/Ca, Na/K and Ca/Mg in the root media. Cumulative uptake of Ca^{2+}, Mg^{2+} and Na^{+} at harvest, for the three growing seasons is presented in Table 7.

Values of C_{kmax} were calibrated with the measured cations concentrations in the above ground maize biomass at different growth stages. The calibrated and validated values of C_{kmax} were estimated at 24.30 μg cm^{-3} for Ca^{2+}, 28.25 μg cm^{-3} for Mg^{2+} and 5.05 μg cm^{-3} for Na^{+}. Computed cumulative uptake of calcium, magnesium and sodium and measured concentrations in plant tissues for the three treatments in 2009, 2010 and 2011 are presented in Fig. 10. Measured and computed values of Ca^{2+} and Mg^{2+} concentration in plant tissues are in agreement with values provided in the literature (Fageria, 2009). The results of the statistical analysis between measured and computed cumulative uptake are given in Table 8.

3.6. Discussion on model calibration and validation results

Ramos et al. (2012) mention that deviations between measured data and simulated values, in model calibration and validation, are mainly attributed to errors related to field measurements, to model input and model structure errors. Deviations between measured and simulated water contents and relatively high *RMSE* values reaching 0.08 cm^{3} cm^{-3} for the layer 95–105 cm (results not shown) can be attributed to the inverse solution estimation of the soil hydraulic properties and possibly errors related to field measurements. For the inverse solution estimation of the soil hydraulic properties with HYDRUS-1D v4.0, measured soil water contents at 10 cm depth were provided for the 0–15 cm soil layer, the measurements at 20 and 30 cm for the 15–35 cm soil layer, at 40 and 60 cm depth for the soil layer 35–90 cm and the soil water recordings at 100 cm were provided for the soil layer 90–110 cm. The simulations seem to describe some layers better than others and some *RMSE* values tend to be high, although the parameter set obtained was the best possible fit ($r^2 = 0.912$) for the entire soil profile of 110 cm. *RMSE* values between measured and computed soil moisture as high as 0.10 and 0.14 cm^{3} cm^{-3} were presented by Schwen et al. (2011) and Valdes-Abellan et al. (2013), respectively. In these studies the soil hydraulic properties of the van Genuchten (1980) model were also estimated by inverse modeling. Therefore, the use of field data for the inverse solution estimation of the soil hydraulic properties does not necessarily guaranty the absolute representativeness of the parameter set, especially for the description of a heterogeneous flow domain of 110 cm, as was the case in this study.

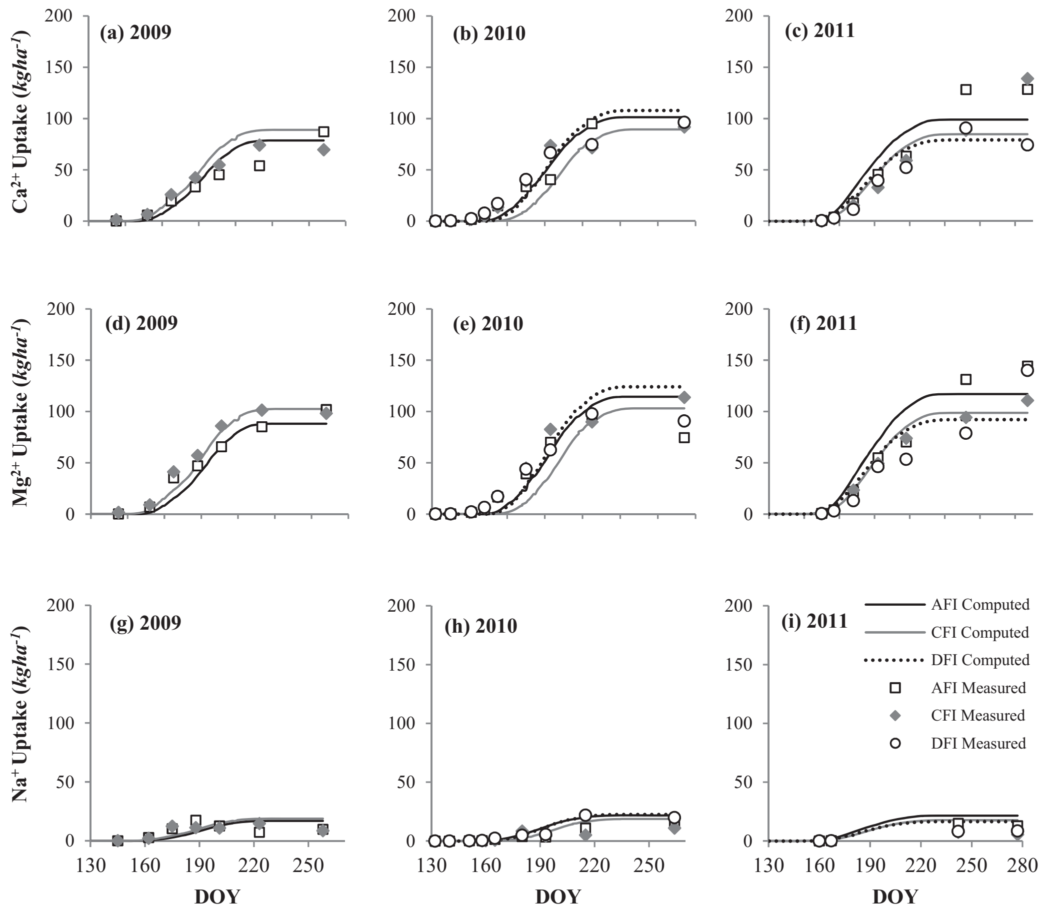

Fig. 10. Computed cumulative uptake and measured concentration of calcium, magnesium and sodium in plant tissues during the three growing periods for the three treatments. DOY denotes Day of Year.

Table 8
Statistical analysis between measured and computed cumulative nutrient uptake obtained for all three treatments (AFI, CFI, DFI).

Nutrient	2009–2010			2011		
	E (kg ha^{-1})	*RMSE* (kg ha^{-1})	*CRM* (–)	*E* (kg ha^{-1})	*RMSE* (kg ha^{-1})	*CRM* (–)
Ca^{2+}	−0.214	11.95	−0.02	0.781	18.76	0.04
Mg^{2+}	−2.624	13.83	0.06	3.218	17.50	−0.06
Na^{+}	1.230	4.71	−0.21	4.814	7.37	−1.12

Errors related to field measurements can be attributed to preferential flow along the soil moisture sensors' access tube walls, even though careful installation procedures were followed. To minimize such possible errors, measuring of soil water content was carried out at least 12 h after an irrigation event which was considered enough time for irrigation water to infiltrate and provide the appropriate balance between the soil and the access tube (Lekakis et al., 2011).

Although the determination of the f_{SP} ratios relies on an easy measured, physically based parameter, which is the saturation percentage of the soil paste, possible source of errors could be related to the determination of EC_{sw} by the $f_{SP}{\cdot}EC_e$ approach. The same approximation applies to the estimation of ions concentration. A major issue in solute transport studies is the sampling method for the determination of soil salinity and cations concentration. Ramos et al. (2011, 2012) refer to spatial soil variability problems encountered in their studies, even with the use of ceramic porous cups for soil solution sampling.

A model structure error could be considered the use of the linear isotherm and the distribution coefficient between the liquid and solid phase, $K_{d,k}$, to describe cation exchange. At present, a major limitation of *WANISIM* model is that it does not account for equilibrium chemical reactions between major ions, such as aqueous complexation, complex cation exchange and precipitation–dissolution. Model UNSATCHEM, which is incorporated in HYDRUS, accounts for such chemical reactions and uses a Gapon-type expression to describe exchange equilibrium between the sorbed and dissolved cations (White and Zelazny, 1986). This approach considers the various interactions between the multiple cations and competition for sorption sites and has proved to be very efficient in modeling the major cations in the soil solution than adsorption isotherms. Recent studies (Ramos et al., 2011; Oster et al., 2012) showed the importance of modeling the major cations using a solute transport model capable of simulating the subsurface transport of multiple ions that mutually interact, create various complex species, compete with each other for sorption sites and/or precipitate or dissolve. Nevertheless, as pointed out by Ramos et al. (2011), the UNSATCHEM module has been used much less often than the standard solute transport module of HYDRUS. This is possibly attributed to the vast number of input parameters and measurements related to soil and chemical factors required for the application. Furthermore, Rasouli et al. (2013) used model UNSATCHEM and concluded that the model performs better for lower than 11.5 dS m^{-1} irrigation water salinity levels.

In this study, higher *RMSE* values between measured and computed cations concentrations were calculated for the DFI treatment and underestimation of the measured values by the model suggests that larger quantities of cations are being adsorbed while less remain in the soil solution, since leaching is limited.

4. Summary and conclusions

The transient-water flow model *WANISIM* was modified to include mass transport of individual ions (Ca^{2+}, Mg^{2+} and Na^{+}) and overall soil salinity. The model calculates EC_{sw} as the sum of the cations in the soil solution, which is more closely related to the chemical processes occurring in the soil, than considering salinity as a single solute. *WANISIM* considers cation exchange and distribution between the liquid and the solid phase however complex ion chemistry is not taken into account.

Data collected during a three year experiment in field plots of maize irrigated with three different irrigation water qualities at Thessaloniki area in Northern Greece, were used for the calibration, validation and evaluation of the model. Visual inspection and the obtained statistical parameters values, suggest relatively good overall correspondence between measured and simulated data of the soil water content, the soil solution electrical conductivity, the concentration of soluble Ca^{2+}, Mg^{2+} and Na^{+} and nutrient uptake. *RMSE* values for cations calculated for AFI (EC_{iw} = 0.8 - dS m^{-1}) and CFI (EC_{iw} = 3.2 dS m^{-1}) treatments were lower than DFI (EC_{iw} = 6.4 dS m^{-1}) treatment, indicating also an underestimation of the measured data, resulting from larger computed cation quantities being adsorbed in the solid phase possibly due to the use of the Freundlich isotherm in its linear form.

Measured and predicted values indicated that the use of saline irrigation waters with EC_{iw} = 3.2 dS m^{-1} and 6.4 dS m^{-1}, caused soil salinization but not sodification in both studied soil layers (0–35 and 35–75 cm). In treatment CFI, EC_{sw} of the surface soil layer, increased significantly from 3.0 dS m^{-1} to approximately 9.0 dS m^{-1} and in treatment DFI from 1.5 to 14.2 dS m^{-1}. Soil salinity was maintained below 4 dS m^{-1}, with the use of the locally available fresh irrigation waters, in AFI treatment.

The peak concentration values of Ca^{2+}, Mg^{2+} and Na^{+} in the treatments were observed in late August–early September periods and the highest values at the end of the last irrigation season. The concentrations subsequently decreased during the rainfall periods in the surface layer. The concentrations of Ca^{2+} and Mg^{2+} gradually increased in the deeper soil layer for DFI and CFI treatments after the first irrigation season. The use of irrigation water with EC_{sw} = 6.4 dS m^{-1} led to high values for Ca^{2+} and Mg^{2+} in the deeper layer of treatment DFI, similar to CFI, within only two irrigation cycles. According to the model results computed leaching losses were limited and high quantities of the applied salts remained in the soil profile of 110 cm.

Measured and computed high concentrations of Ca^{2+} and Mg^{2+} compared to Na^{+} in the irrigation water and the soil solution, did not lead to soil sodification, thus maintaining *SAR* values below 4 $(mmol_{(c)}\,L^{-1})^{0.5}$ in all treatments, during the three year experiment.

Root water uptake reductions due to water and osmotic stress were also predicted by model *WANISIM*. Due to water stress, transpiration was reduced by approximately 21% in AFI and CFI and 24% in DFI treatment. Under combined water and osmotic stress, root water uptake was further reduced by 0.2% in AFI, 0.7% in CFI and 0.4% in DFI. Limited root water uptake reductions under osmotic stress were attributed to the increased plant salt tolerance due to reduced soil moisture, that maintained water uptake in the dry periods between irrigations.

Model *WANISIM* introduces the approach of the f_{SP} ratio which takes into account the effects of soil moisture on plant salt tolerance. The f_{SP} ratio is a physically based parameter and is multiplied by the threshold salinity of the plants. The ratio is higher in low moisture levels and the threshold salinity increases, increasing plant salt tolerance in drier conditions. Model results reveal that water uptake continued in small amounts in the dry periods between irrigations in deeper than 15 cm soil layers for treatments CFI and DFI, compensating in this way the reductions in water uptake due to osmotic stress.

The model can further be improved with the incorporation of modules that account for various interactions between cations in the liquid and solid phase. However, comparison with results from previous studies that used models accounting for chemical equilibrium proved that a medium structure model like *WANISIM* can predict with an acceptable accuracy cations concentrations in the soil solution, salinity and sodicity. Furthermore, this approach presents fewer requirements in input parameters than models employing complex processes of adsorption and cation exchange.

WANISIM can be used for irrigation management in regions with scarce water resources and low quality water available for irrigation, to describe the effects of irrigation water quality on soil and water uptake by plants.

Acknowledgments

The financial support of this research by Greek Scholarship Foundation (IKY) is gratefully acknowledged.

References

Allen, R.G., Walter, I.A., Elliott, R., Howell, T., Itenfisu, D., Jensen, M., 2005. The ASCE standardized reference evapotranspiration equation. Final Report (ASCE-EWRI). Pr. In: Allen, R.G., Walter, I.A., Elliott, R., Howell, T., Itenfisu, D., Jensen, M. (Eds.), Environmental and Water Resources Institute, 2005. Task Committee on Standardization of Reference Evapotranspiration of the Environmental and Water Resources Institute.

Allison, L.E., Moodie, C.D., 1965. Carbonates. In: Black, C.A. (Ed.), Methods of Soil Analysis. Part 2. Agronomy Monograph. American Society of Agronomy, Madison, WI, pp. 1379–1400.

Antonopoulos, V.Z., 1997. Simulation of soil moisture dynamics on irrigated cotton in semiarid climates. Agric. Water Manage. 34, 233–246.

Antonopoulos, V.Z., 2000. Modeling of soil water dynamics in an irrigated corn field using direct and pedotransfer functions for hydraulic properties. Irrig. Drain. Syst. 14, 325–342.

Antonopoulos, V.Z., 2001. Simulation of water and nitrogen balances of irrigated and fertilized corn-crop soil. J. Irrig. Drain. Eng. ASCE 127 (2), 77–83.

Antonopoulos, V.Z., 2006. Water movement and heat transfer simulations in a soil under ryegras. Biosyst. Eng. 95, 127–138.

Antonopoulos, V.Z., Papazafiriou, Z.G., 1990. Solutions of one-dimensional water flow and mass transport equations in variably saturated porous media by the finite element method. J. Hydrol. 119, 151–167.

Antonopoulos, V.Z., Wyseure, G.C.L., 1998. Modeling of water and nitrogen dynamics on an undisturbed soil and a restored soil after open-cast mining. Agric. Water Manage. 37, 21–40.

APHA, 2005. Standard methods for the examination of water and wastewater. Centennial edition. In: Eaton, A.D., Clesceri, L.S., Rice, E.W., Greenberg, A.E. (Eds.), 21st ed, APHA, AWWA, WEF, Washington.

Aschonitis, V.G., Kostopoulou, S.K., Antonopoulos, V.Z., 2012. Methodology to assess the effects of rice cultivation under flooded conditions on van Genuchten's model parameters and pore size distribution. Transp. Porous Med. 91, 861–876.

Aschonitis, V.G., Papamichail, D.M., Lithourgidis, A., Fano, E.A., 2014. Estimation of leaf area index and foliage area index of rice using an indirect gravimetric method. Commun. Soil Sci. Plant Anal. 45 (13), 1726–1740.

Ayers, R.S., Westcot, D.W., 1985. Water Quality for Agriculture. Irrig. Drain. Pap. 29, FAO, Rome, Italy.

Belmans, C., Wesseling, J.G., Feddes, R.A., 1983. Simulation model of the water balance of a cropped soil: SWATRE. J. Hydrol. 63, 271–286.

Biggar, J.W., Nielsen, D.R., 1976. Spatial variability of the leaching characteristics of a field soil. Water Resour. Res. 12, 78–84.

Bonfante, A., Basile, A., Acutis, M., De Mascellis, R., Manna, P., Perego, A., Terribile, F., 2010. SWAP, CropSyst and MACRO comparison in two contrasting soils cropped with maize in Northern Italy. Agric. Water Manage. 97 (7), 1051–1062.

Bouyoucos, G.J., 1962. Hydrometer method improved for making particle size analysis of soils. Agron. J. 54, 464–465.

Bresler, E., Mc Neal, B.L., Carter, D.L., 1982. Saline and Sodic Soils (Principles–Dynamics–Modeling). Springer-Verlag, New York.

Dioudis, P.S., Filintas, A.T., Papadopoulos, A.H., 2009. Corn yield response to irrigation interval and the resultant savings in water and other overheads. Irrig. Drain. 58 (1), 96–104.

Donohue, S.J., Aho, D.W., 1992. Determination of P, K, Ca, Mg, Mn, Fe, Al, B, Cu, and Zn in plant tissue by Inductively Coupled Plasma (ICP) Emission Spectroscopy.

In: Plank, C.O. (Ed.), Plant analysis reference procedures for the southern region of the United States. Southern Cooperative Series Bulletin 368. The University of Georgia. Crop and Soil Science Dept., Athens, pp. 34–37.
Doorenbos, J., Pruitt, W.O., 1977. Crop Water Requirements. Irrig. and Drain. Pap. 24, FAO, Rome, Italy.
Fageria, N.K., 2009. The Use of Nutrients in Crop Plants. Taylor and Francis Group, LLC, CRC Press, Boca Raton.
Feddes, R.A., Kowalik, P.J., Zaradny, H., 1978. Simulation of field water use and crop yield. Simulation Monographs. Pudoc, Wageningen.
Feddes, R.A., Raats, P.A.C., 2004. Parameterizing the soil–water–plant root system. In: Feddes, R.A., de Rooij, G.J., van Dam, J.C. (Eds.), Unsaturated-zone Modeling: Progress, Challenges and Applications. Wageningen UR Frontis Series, vol. 6. Kluwer Academic Publishers, Dordrecht, the Netherlands, pp. 95–141.
Georgiou, P.E., Antonopoulos, V.Z., Lekakis, E.H., 2010. Soil water balance and distribution in a field of maize under partial root-zone drying drip irrigation. In: e-Proceedings of the International Conference PRE10 Protection and Restoration of the Environment X, Corfu, Greece, p. 8.
Ghassemi, F., Jakeman, A.J., Nix, H.A., 1995. Salinisation of Land and Water Resources. University of New South Wales Press Ltd., Canberra, Australia.
Gonçalves, M.C., Šimůnek, J., Ramos, T.B., Martins, J.C., Neves, M.J., Pires, F.P., 2006. Multicomponent solute transport in soil lysimeters with waters of different quality. Water Resour. Res. 42, W08401. http://dx.doi.org/10.1029/2005WR004802.
Grattan, S.R., Oster, J.D., Benes, S.E., Kaffka, S.R., 2012. Use of saline drainage waters for irrigation. In: Wallender, W.W., Tanji, K.K. (Eds.), Agricultural Salinity Assessment and Management, second ed., ASCE Manuals and Reports on Engineering Practice No. 71. ASCE, Reston, VA, pp. 687–720.
Homaee, M., Dirksen, C., Feddes, R.A., 2002. Simulation of root water uptake. I. Non-uniform transient salinity using different macroscopic reduction functions. Agric. Water Manage. 57 (2), 89–109.
Hopmans, J.W., Šimůnek, J., Romano, N., Durner, W., 2002. Inverse modeling of transient water flow. In: Dane, J.H., Topp, G.C. (Eds.), Methods of Soil Analysis, Part 1, Physical Methods, Chapter 3.6.2, 3rd ed. SSSA, Madison, WI, pp. 963–1008.
Huyakorn, P.S., Thomas, S.D., Thompson, B.M., 1984. Techniques for making finite elements competitive in modeling flow in variably saturated porous media. Water Resour. Res. 20, 1099–1115.
Jarvis, N.J., Brown, C.D., Granitza, E., 2000. Sources of error in model predictions of pesticide leaching: a case study using the MACRO model. Agric. Water Manage. 44 (1–3), 247–262.
Kang, S., Zhang, F., Zhang, J., 2001. A simulation model of water dynamics in winter wheat field and its application in a semiarid region. Agric. Water Manage. 49, 115–129.
Kang, S.Z., Gu, B.J., Du, T.S., Zhang, J.H., 2003. Crop coefficient and ratio of transpiration to evapotranspiration of winter wheat and maize in a semi-humid region. Agric. Water Manage. 59, 239–254.
Kargas, G., Kerkides, P., Poulovassilis, A., 2012. Infiltration of rain water in semi-arid areas under three land surface treatments. Soil Tillage Res. 120, 15–24.
Kargas, G., Kerkides, P., Seyfried, P.M., Sgoumbopoulou, A., 2011. WET sensor performance in organic and inorganic media with heterogeneous moisture distribution. Soil Sci. Soc. Am. J. 75 (4), 1244–1252.
Kroes, J.G., van Dam, J.C., Huygen, J., Vervoort, R.W., 1999. User's Guide of SWAP version 2.0; Simulation of water flow, solute transport and plant growth in the Soil–Water–Atmosphere–Plant environment. Wageningen Agricultural University. Report 81, DLO Winand Staring Centre. Technical Document 53, pp. 128.
Kutilek, M., Nielsen, D.R., 1994. Soil Hydrology. GeoEcology Textbook. Catena Verlag, Germany.
Lekakis, E.H., Georgiou, P.E., Pavlatou-Ve, A., Antonopoulos, V.Z., 2011. Effects of fixed partial root-zone drying irrigation and soil texture on water and solute dynamics in calcareous soils and corn yield. Agric. Water Manage. 101, 71–80.
Letey, J., 2007. Guidelines for irrigation management of saline waters are overly conservative. In: Zaidi, M.K. (Ed.), Wastewater reuse – risk assessment, decision-making and environmental security. Proceedings of the NATO Advanced Research Workshop on wastewater reuse – risk assessment, decision-making and environmental security. Istanbul, Turkey, 12–16 October 2006. Series: NATO Science for Peace and Security Series C: Environmental Security, pp. 205–218.
Loague, K., Green, R., 1991. Statistical and graphical methods for evaluating solute transport models: overview and applications. J. Contam. Hydrol. 7, 51–73.
Läuchli, A., Grattan, S.R., 2007. Plant growth and development under salinity stress. In: Jenks, M.A., Hasegawa, P.M., Jain, S.M. (Eds.), Advances in Molecular Breeding toward Drought and Salt Tolerant Crops. Springer, Dordrecht, the Netherlands, pp. 1–32.
Maas, E.V., 1996. Crop salt tolerance. In: Tanji, K.K. (Ed.), Agricultural Salinity Assessment and Management. ASCE Manual and Report on Engineering Practice No. 71 (corrected edition), Am. Soc. of Civ. Eng., New York, pp. 262–304.
Maas, E.V., Hoffman, G.J., 1977. Crop salt tolerance – current assessment. J. Irrig. Drain. Div. ASCE 103 (IR2), 115–134.
Mertens, J., Stenger, R., Barkle, G.F., 2006. Multiobjective inverse modeling for soil parameter estimation and model verification. Special section: Parameter identification and uncertainty assessment in the unsaturated zone. Vadose Zone J. 5, 917–933.
Miller, J.J., Curtin, D., 2008. Electrical conductivity and soluble ions. In: Carter, M.R., Gregorich, E.G. (Eds.), Soil sampling and methods of analysis. Canadian Society of Soil Science, second ed. CRC Press, Taylor & Francis Group, Boca Raton, pp. 161–171.
Oster, J.D., Letey, J., Vaughan, P., Wu, L., Qadir, M., 2012. Comparison of transient state models that include salinity and matric stress effects on plant yield. Agric. Water Manage. 103, 167–175.
Pang, X.P., Letey, J., 1998. Development and evaluation of ENVIRO-GRO, an integrated water, salinity, and nitrogen model. Soil Sci. Soc. Am. J. 62, 1418–1427.
Papazafiriou, Z.G., 1996. Crop evapotranspiration: regional studies in Greece. In: Proceedings of International Symposium of Applied Agrometeorology and Agroclimatology, European Commission, COST 77, 79, 711, EUR 18328, pp. 275–286.
Pitman, M.G., Läuchli, A., 2002. Global impact of salinity and agricultural ecosystems. In: Läuchli, A., Lüttge, U. (Eds.), Salinity: Environment–Plants–Molecules. Kluwer Academic Publishers, Dordrecht, pp. 3–20.
Profile Probe User Manual 2.0. Version: PR2-UM-2.0 December 2004. Delta-T Devices Ltd., UK.
Qadir, M., Oster, J.D., 2004. Crop and irrigation management strategies for saline sodic soils and waters aimed at environmentally sustainable agriculture. Sci. Total Environ. 323, 1–19.
Qadir, M., Sharma, B.R., Bruggeman, A., Choukr-Allah, R., Karajeh, F., 2007. Nonconventional water resources and opportunities for water augmentation to achieve food security in water scarce countries. Agric. Water Manage. 87, 2–22.
Ragab, R., 2002. A holistic generic integrated approach for irrigation, crop and field management: the SALTMED model. Environ. Model. Softw. 17, 345–361.
Rahil, M.H., Antonopoulos, V.Z., 2007. Simulating soil water flow and nitrogen dynamics in a sunflower field irrigated with reclaimed wastewater. Agric. Water Manage. 92, 142–150.
Ramos, T.B., Šimůnek, J., Gonçalves, M.C., Martins, J.C., Prazeres, A., Castanheira, N.L., Pereira, L.S., 2011. Field evaluation of a multicomponent solute transport model in soils irrigated with saline waters. J. Hydrol. 407, 129–144. http://dx.doi.org/10.1016/j.jhydrol.2011.07.016.
Ramos, T.B., Šimůnek, J., Gonçalves, M.C., Martins, J.C., Prazeres, A., Pereira, L.S., 2012. Two-dimensional modeling of water and nitrogen fate from sweet sorghum irrigated with fresh and blended saline waters. Agric. Water Manage. 111, 87–104.
Rasouli, F., Pouya, A.K., Šimůnek, J., 2013. Modeling the effects of saline water use in wheat-cultivated lands using the UNSATCHEM model. Irrig. Sci. 31, 1009–1024.
Rhoades, J.D., 1996. Salinity: electrical conductivity and total dissolved solids. In: Sparks, D.L., et al. (Ed.), Methods of Soil Analysis. Part 3 – Chemical Methods. Soil Science Society of America Book Series 5. Soil Sci. Soc. Am., Am. Soc. Agron. Madison, WI, pp. 417–436.
Rowe, R.K., Badv, K., 1996. Chloride migration through clayey silt underlain by fine sand or silt. J. Geotech. Eng. 122 (1), 60–68.
Schwen, A., Bodner, G., Loiskandl, W., 2011. Time-variable soil hydraulic properties in near-surface soil water simulations for different tillage methods. Agric. Water Manage. 99, 42–50.
Shani, U., Dudley, L.M., 2001. Field studies of crop response to drought and salt stress. Soil Sci. Soc. Am. J. 65, 1522–1528.
Šimůnek, J., Hopmans, J.W., 2009. Modeling compensated root water and nutrient uptake. Ecol. Model. 220, 505–521.
Šimůnek, J., Šejna, M., Saito, H., Sakai, M., van Genuchten, M.Th., 2008. The HYDRUS-1D software package for simulating the movement of water, heat, and multiple solutes in variably-saturated media. Version 4.0. HYDRUS Software Series 3, Department of Environmental Sciences, University of California Riverside, Riverside, CA, USA, 315pp.
Šimůnek, J., Suarez, D.L., Šejna, M., 1996. The UNSATCHEM software package for simulating one-dimensional variably saturated water flow, heat transport, carbon dioxide production and transport, and multicomponent solute transport with major ion equilibrium and kinetic chemistry. Version 2.0, Res. Rep. 141, US Salinity Lab., Agric. Res. Serv., Riverside, Calif., pp. 186.
Skaggs, T.H., Shouse, P.J., Poss, J.A., 2006. Irrigating forage crops with saline waters: 2. Modeling root uptake and drainage. Vadose Zone J. 5, 824–837.
Thomas, G.W., 1982. Exchangeable cations. In: Klute, A. (Ed.), Methods of soil analysis. Part 2. Chemical and microbiological properties, second ed., Agronomy Monograph 9. Am. Soc. Agron., Soil Sci. Soc. Am., Madison, WI, USA, pp. 159–165.
Tinker, P.B., Nye, P.H., 2000. Solute Movement in the Rhizosphere. Oxford University Press, New York, USA, p. 444.
U.S. Salinity Laboratory Staff, 1954. Diagnosis and improvement of saline and alkali soils. United States Department of Agriculture, Washington. Agriculture Handbook/USDA No. 60.
U.S.EPA (U.S. Environmental Protection Agency), 1999. Understanding Variation in Partition Coefficient, Kd, Values, Volume I: The Kd Model, Methods of Measurement, and Application of Reaction Codes. Office of Air and Radiation, U.S.EPA 402-R-99-004A, Washington D.C., 326 p.
Valdes-Abellan, J., Jiménez-Martínez, J., Candela, L., 2013. HYDRUS application to assess possible impacts of non-conventional water irrigation under two different vadose zone monitoring strategies. In: Šimůnek, J., van Genuchten, M.Th., Kodešová, R. (Eds.), Proceedings of the 4th International Conference "HYDRUS Software Applications to Subsurface Flow and Contaminant Transport Problems". Dept. of Soil Science and Geology, Czech University of Life Sciences, Prague, Czech Republic, March 21–22, 2013, pp. 377–384, ISBN: 978-80-213-2380-3.

van Genuchten, M.T., 1980. A closed form equation for predicting the hydraulic conductivity of unsaturated soils. Soil Sci. Soc. Am. J. 44, 892–898.
Walkley, A., Black, I.A., 1934. An examination of the Degtjareff method for determining soil organic matter, and a proposed modification of the chromic acid titration method. Soil Sci. 37, 29–38.
Wesseling, J.G., Elbers, J.A., Kabat, P., van den Broek, B.J., 1991. SWATRE: instructions for input. Internal Note. Winand Staring Centre, Wageningen, the Netherlands.
White, N.L., Zelazny, L.M., 1986. Charge properties in soil colloids. In: Sparks, D.L. (Ed.), Soil Physical Chemistry. CRC Press, Boca Raton, pp. 39–81.
WMO (World Meteorological Organization), 2008. Guide to Meteorological Instruments and Methods of Observation, second ed., WMO Publications, Switzerland (Chapter 11).
Yurtseven, E., Šimůnek, J., Avcı, S., Öztürk, H.S., 2013. Comparison of HYDRUS-1D simulations and ion (salt) movement in the soil profile subject to leaching. In: Šimůnek, J., van Genuchten, M.Th., Kodešová, R. (Eds.), Proceedings of the 4th International Conference "HYDRUS Software Applications to Subsurface Flow and Contaminant Transport Problems", Dept. of Soil Science and Geology, Czech University of Life Sciences, Prague, Czech Republic, March 21–22, 2013, pp. 395–404, ISBN: 978-80-213-2380-3.